ULTRASOUND-MEDIATED DEGRADATION OF XANTHAN POLYMER IN AQUEOUS SOLUTION: ITS SCISSION MECHANISM AND THE EFFECT OF SODIUM CHLORIDE INCORPORATION

HAZIQAH BINTI MOHD SALEH

FACULTY OF SCIENCE
UNIVERSITY OF MALAYA
KUALA LUMPUR

2017

ULTRASOUND-MEDIATED DEGRADATION OF XANTHAN POLYMER IN AQUEOUS SOLUTION: ITS SCISSION MECHANISM AND THE EFFECT OF SODIUM CHLORIDE INCORPORATION

HAZIQAH BINTI MOHD SALEH

DISSERTATION SUBMITTED IN FULFILMENT OF THE REQUIREMENTS FOR THE DEGREE OF MASTER SCIENCE

INSTITUTE OF BIOLOGICAL SCIENCES
FACULTY OF SCIENCE
UNIVERSITY OF MALAYA
KUALA LUMPUR

2017

UNIVERSITI MALAYA

ORIGINAL LITERARY WORK DECLARATION

Name of Candidate : **HAZIQAH BINTI MOHD SALEH**

I.C/Passport No

Registration/Matric No : **SGR 120070**

Name of Degree : **MASTER OF SCIENCE**

Title of Project Paper/Research Report/Dissertation/Thesis ("this Work"):

ULTRASOUND-MEDIATED DEGRADATION OF XANTHAN POLYMER IN AQUEOUS SOLUTION: ITS SCISSION MECHANISM AND THE EFFECT OF SODIUM CHLORIDE CONCENTRATION

Field of Study : **APPLIED MICROBIOLOGY**

I do solemnly and sincerely declare that:

(1) I am the sole author/writer of this Work;
(2) This Work is original;
(3) Any use of any work in which copyright exists was done by way of fair dealing and for permitted purposes and any excerpt or extract from, or reference to or reproduction of any copyright work has been disclosed expressly and sufficiently and the title of the Work and its authorship have been acknowledged in this Work;
(4) I do not have any actual knowledge nor do I ought reasonably to know that the making of this work constitutes an infringement of any copyright work;
(5) I hereby assign all and every rights in the copyright to this Work to the University of Malaya ("UM"), who henceforth shall be owner of the copyright in this Work and that any reproduction or use in any form or by any means whatsoever is prohibited without the written consent of UM having been first had and obtained;
(6) I am fully aware that if in the course of making this Work I have infringed any copyright whether intentionally or otherwise, I may be subject to legal action or any other action as may be determined by UM.

Candidate's Signature: Date:

Subscribed and solemnly declared before,

Witness's Signature: Date:
Name:
Designation:

ABSTRACT

Xanthan gum is a versatile polymer with a wide range of industrial applications. The natural extracellular polymer is synthesized by *Xanthomonas* sp. from renewable resources. It exhibits superior properties to be used as thickener and stabilizer for emulsions and suspensions. Nonetheless, xanthan gum is practically limited by its own very high molecular weight for specific types of applications such as nano-sized emulsion. Hence, for an even wider range of uses, tailored functionalization through degradation is key to further expand its functionality hence adding more values to the industrial worth polymer. In this study, degradation of xanthan gum in aqueous solution by ultrasonic irradiation was investigated. Ultrasound-mediated process is highly advantageous over other degradation methods such as chemical since it employs acoustic wave to carry out the hydrolysis. Consequently, downstream processing complications in separation and purification steps are drastically minimized. Four sonication parameters were selected to be investigated and optimized in this study *viz.* sonication intensity, irradiation time, concentration of xanthan gum and molar concentration of NaCl solution. Combined approach of full factorial design and conventional one-factor-at-a-time was applied to obtain the optimum degradation of xanthan polymer. Using degree of degradation (%) as a response, optimum degradation was achieved at sonication power intensity of 11.5 W cm^{-2}, irradiation time 120 min and 0.1 g L^{-1} xanthan in salt-free solution. Molecular weight reduction of xanthan under sonication was also investigated. The degradation behaviour followed second-order exponential decay function with two different rate constants obtained for different segments of the curve. Molecular weight reduction rate constant of 14.6×10^{-2} s^{-1} was determined for the early phase of irradiation, while a slower rate constant of 6.1×10^{-4} s^{-1} was calculated for a later phase. The limiting molecular weight where fragments no longer undergo scission was also determined from the function. Different limiting

molecular weight was observed with respect to sonication conditions where the incorporation of NaCl in xanthan aqueous solution resulted in higher limiting molecular weight. Different scission models were proposed i.e random- and mid-point chain scission models. The ultrasound-mediated degradation of aqueous xanthan polymer agreed with mid-point scission model, and was supported by the molecular weight analysis and thermal decomposition behaviour of sonicated xanthan gum. Side chain of xanthan polymer was proposed to be the primary site of scission action.

ABSTRAK

Gam xanthan merupakan polimer serbaguna untuk aplikasi-aplikasi dalam pelbagai bidang industri. Polimer luar sel semulajadi ini disintesis oleh *Xanthomonas* sp. daripada sumber yang boleh diperbaharui. Ia menunjukkan ciri – ciri unggul untuk digunapakai sebagai pemekat dan penstabil di dalam emulsi dan ampaian. Walau bagaimanapun, gam xanthan dihadkan secara praktis oleh berat molekul yang sangat besar bagi aplikasi spesifik seperti emulsi saiz nano. Maka, untuk kegunaan yang lebih meluas, fungsian terarah melalui degradasi adalah kunci kepada melebarkan kebolehfungsiannya, dan seterusnya meningkatkan lagi nilai industrinya. Di dalam kajian ini, degradasi gam xanthan di dalam larutan akues oleh pemancaran lampau bunyi telah disiasat. Proses berasaskan lampau bunyi mempunyai kelebihan besar jika dibandingkan dengan kaedah degradasi yang lain seperti kimia kerana ianya hanya menggunakan gelombang bunyi untuk melaksanakan proses hidrolisis. Oleh itu, komplikasi proses hiliran dalam pemisahan dan penulinan diminimakan secara drastik. Empat parameter lampau bunyi telah dipilih untuk dikaji dan seterusnya dioptimumkan iaitu keamatan lampau bunyi, tempoh pemancaran, kepekatan gam xanthan dan kepekatan molar larutan NaCl. Gabungan antara kaedah rangka eksperimen secara rekabentuk faktor lengkap (FFD) dan satu-faktor-satu-masa telah digunapakai untuk mendapatkan tahap optima degradasi polimer xanthan. Dengan menggunakan tahap degradasi (%) sebagai respon, degradasi optima diperolehi pada keamatan kuasa lampau bunyi 11.5 W cm^{-2}, tempoh pemancaran selama 120 min, dan kepekatan xanthan 0.1 g L^{-1} di dalam larutan bebas garam. Pengurangan berat molekul xanthan semasa lampau bunyi juga dikaji. Pola degradasi mematuhi fungsi pereputan eksponen darjah kedua dengan dua kadar pereputan telah dikenalpasti berdasarkan segmen-segmen berbeza lengkungan tersebut. Pada peringkat awalnya, pemalar kadar pereputan ditentukan pada 14.6×10^{-2} s^{-1}, manakala pemalar kadar pereputan yang lebih perlahan iaitu 6.1×10^{-4} s^{-1}

di peringkat seterusnya. Berat molekul penghad di mana fragmen polimer tidak lagi melalui pemotongan juga dapat ditentukan daripada fungsi tersebut. Had berat molekul yang berbeza telah didapati berdasarkan keadaan lampau bunyi di mana kehadiran NaCl di dalam larutan akues xanthan telah menghasilkan berat molekul penghad yang lebih tinggi. Dua model pemotongan rantaian polimer telah dicadangkan iaitu pemotongan rantaian polimer pada bahagian tengah dan potongan rantaian polimer secara rawak. Degradasi diperantarakan oleh lampau bunyi mematuhi model potongan pada bahagian tengah, dan ini disokong oleh analisa berat molekul dan kelakuan penguraian termal gam xanthan yang telah dilampau bunyi. Rantai sisi polimer xanthan dicadangkan sebagai kedudukan primer tindakan pemotongan.

ACKNOWLEDGMENTS

Alhamdulillah, all praise to Allah the most merciful for guiding me to the end of this winding journey, granting me with unbelievable strength, endless hopes and opportunities in completing this research.

First and foremost, I would like to convey my heartfelt gratitude and sincere appreciation to all wonderful people that I met along the way especially to the most important person, Professor Dr. M. Suffian M. Annuar that always committed and patient in supervising and guiding me through this challenging phase. I also owe a debt of gratitude to Dr Khanom Simarani for her countless support and encouragement. Without these excellent people, this study would not have been successful.

My deepest appreciation to B.E.T and B.A.M members; Kak Nadiah, Kak Faizah, Kak Syairah, Kak Ana, Hindartu, Kak Suhayati, Kak Farah, Rafiah, Ira, Juwaini, Haziq, Abang Nazis, Chuck, Abang Rafais and Chong Boon who always have been helpful and encouraging.

Special thanks to my family that understand me the most, and showering me with unending support and love during this project completion. To these important people that have become my pillar of strength; Ema, Izlin and Farheen, thank you for making this journey worth a lifetime of memories.

Last but not least. Thank you to all who supported and helped. Your kind words and gestures keep me moving forward. I truly treasured the memories, friendship and knowledge that I made along this way.

TABLE OF CONTENTS

LIST OF FIGURES

LIST OF TABLES

LIST OF ABBREVIATIONS

NaCl	Sodium chloride
IPA	Isopropyl alcohol
DNS	Dinitrosalicyclic acid
KCl	Potassium chloride
NaOH	Sodium hydroxide
TFA	Trifluoroacetic acid
H_2SO_4	Sulphuric acid
KOH	Sodium hydroxide
$BaCO_3$	Barium carbonate
DPPH	Hydroxyl radical, 2,2-diphenyl-1-picrylhydrazyl
LLA	α-linolenic acid
sp.	species
CMC	carboxymethylcellulose
D_2O	Deuterated water
g	Gram
mg	Miligram
cm	Centimeter
M	Molar
kHz	Kilohertz
K	Kelvin
°C	Degree celcius
s	Second
min	Minute
W	Watt
Atm	Atmosphere
MHz	Megahertz
mL	Mililtre
µL	Microlitre
l	Litre
m	Mass
nm	Nanometer
Da	Dalton

Rpm	Rotating per minute
C_p	Specific heat capacity of water
mPa.s	Milipascal
I	Intensity
(ΔH_v)	enthalpy of vaporization
P_v	liquid vapour pressure
(σ)	Surface tension
L_c	Contour length
L_p	Persistence length
RMSD	Root mean square
F	F-statistic
P	P-statistic
FFD	Full factorial design
OD	Optical density
ANOVA	Analysis of variance
SEC	Size exclusion chromatography
TGA	Thermogravimetric Analysis
*d*TGA	Derivative Thermogravimetric Analysis
DSC	Differential Scanning Calorimetry
FTIR	Fourier-Transform Infrared Spectroscopy
^{1}H NMR	Proton nuclear magnetic resonance

CHAPTER 1

INTRODUCTION

Xanthan gum has long been widely applied in industries and research. Despite the ever-growing new discoveries, this microbial biopolymer still garners major attention due to its continuously expanding applicability. Xanthan gum has been linked to applications that range from food (Sharma *et al.*, 2006), agricultural (Palaniraj & Jayaraman, 2011), pharmaceutical, cosmetics (Benny *et al.*, 2014; Zatz, 1984) to the utilization in petroleum industries (Navarrete *et al.*, 2000; Sandvik & Maerker, 1977) . Its well known properties of high solubility and stability over a wide range of pH and temperature, high viscosity and compatibility with many others substances (Kalogiannis *et al.*, 2003) have all been documented. However, emerging novel applications of xanthan-derived oligosaccharides as antioxidants (Wu *et al.*, 2013; Xiong *et al.*, 2013; Xiong *et al.*, 2014), elicitor (Liu *et al.*, 2005) and antibacterial agents (Qian *et al.*, 2006) are yet to be fully explored.

Due to its versatility, the utilization of xanthan gum is expanding and many studies are continuously been carried out to unleash its full potentials. However, due to its very high molecular weight and massive molecular size somehow become a limiting factor for many other potential applications. Therefore, it is proposed for xanthan gum to be modified by reducing its size and molecular weight *via* controlled degradation, which offers tailored functionalization to xanthan gum. Controlled degradation not only expands xanthan gum functionalities, it would also add more values to the resulting products as platform chemicals compared to native xanthan gum.

Many degradations attempts have been carried out in order to effectively obtain controlled xanthan gum degradation. Xanthan gum has been degraded chemically (Christensen *et al.*, 1996; Christensen & Smidsrød, 1991; Christensen *et al.*, 1993; Stokke & Christensen, 1996), enzymatically (Cheetham & Mashimba, 1991; Kool *et al.*, 2014) and by thermal exposure (Lambert & Rinaudo, 1985). However, the drawbacks of these methods e.g. addition of other chemical reagents, not environmental-friendly, slow process, purification complication, by-products formation among others, necessitate the search for an alternative degradation method. Ultrasound-mediated degradation has become a promising alternative of great benefits since it is greener, rapid, energy saving, effective and by product-free (Liu *et al.*, 2006; Wu *et al.*, 2008). To date, only a few studies reported on ultrasonic degradation of xanthan gum i.e. from Li and Feke (2015), Tiwari *et al.* (2010) and Milas *et al.* (1986). Even then, only limited aspects have been investigated and the critical features of the degradation process have not thoroughly been discussed.

Therefore, the present study sought to investigate the prominent aspect of degradation using ultrasonic irradiation. Selected ultrasound-mediated degradation parameters will be investigated and optimized i.e. concentration of xanthan gum in aqueous solution, sonication intensity, irradiation time and NaCl concentration in the solution. The effect of salt inclusion will be investigated because it was hypothesized to enhance the efficiency of xanthan gum degradation under acoustic pressure (Li & Feke, 2015), thus the ability to manipulate this particular variable would provide a simple mean to control the degradation process. An appropriate scission model will also be proposed alongside the site of scission action.

A better understanding of key factors that will enhance the efficiency of this process and insight into some fundamental aspects of ultrasound-mediated degradation of xanthan polymer obtained from the present research is anticipated to guide further

development, discoveries and invention on both xanthan gum application and ultrasonic processing in the future.

The objectives of this study are:

1) To study the effects of selected sonication process parameters towards xanthan gum degradation;
2) To optimize the selected sonication process parameters in order to increase the degradation efficiency;
3) To investigate the effects of NaCl inclusion in aqueous xanthan gum solution towards the ultrasound-mediated degradation;
4) To propose the scission mechanism of xanthan gum under ultrasonic irradiation.

CHAPTER 2

LITERATURE REVIEW

2.1 XANTHAN GUM

2.1.1 Xanthan gum

Xanthan gum is a natural microbial polysaccharide excreted by plant pathogenic bacteria of *Xanthomonas* genus. A well-known producer of xanthan gum is *Xanthomonas campestris*. *Xanthomonas* sp. is Gram negative, rod-shaped with single polar flagellum and an obligate aerobe, exhibiting yellow, smooth and viscid colonies (He & Zhang, 2008; Vicente & Holub, 2013).These bacteria infect plants from *Brassicacae* family e.g. cabbages, lettuces and cauliflowers by causing black rot diseases (Lu *et al.*, 2007). Black rot is a systemic vascular disease. The typical disease symptoms include blackening of the veins and V-shaped yellow lesions starting from the leaf margins (Vicente & Holub, 2013). Xanthan gum is the capsular polysaccharide that is loosely attached to the bacterial cell. This virulence factor protects the bacteria from environmental stresses and aid during the infection process (Hsiao *et al.*, 2005).

2.1.2 Xanthan gum production

Xanthan gum, the first industrially produced biopolymer was first discovered in the 1950s at the Northern Regional Research Laboratories (NRRL) of the United States Department of Agriculture followed by mass commercial production in early 1964. Good preservation and maintenance technique need to be applied to prevent degeneration of the bacterial strain during the upstream process due to the inability of degenerated strain, labelled as V_s (very small) in producing xanthan gum. A non viscid pale yellow colonies, V_s strain is formed from the degradation of old culture *L* (large) strain (García-Ochoa *et al.*, 2000).

Since xanthan gum constitutes the bacterial capsule, xanthan gum production is growth associated. However, increases in cell concentration resulted in high production of xanthan that impedes mass transport of nutrients and prolonging the lag phase of cell growth. Therefore, multiple stages of inoculum development are employed to suppress xanthan production while building up the cell mass (Sharma *et al.*, 2014). Glucose and sucrose are the favourite carbon source in most commercial xanthan gum production. Operation is usually carried out in batch culture fermentation at temperature of approximately 28 – 30 °C, pH ~ 7 and aeration rate of higher than 0.3 (v/v). The fermentation process is carried out for about 100 hour and converts an approximately 50 % of glucose substrate into xanthan product (García-Ochoa *et al.*, 1997; Leela & Sharma, 2000; Mirik *et al.*, 2011; Souw & Demain, 1979).

The downstream process of xanthan gum production is the most challenging part. The recovery process of xanthan gum from fermentation broth at the end of production is difficult and expensive due to the highly viscous broth (García-Ochoa *et al.*, 2000). Therefore, the specific purification method is determined by demands from the consumers. When industrial grade xanthan is required, the fermented broth is pasteurized to deactivate enzyme(s) present and sterilized the bacteria (Smith & Pace, 1982). Xanthan gum is then precipitated using large amount of alcohol followed by spray drying. This hydrophilic polymer formed a true solution in water (Smith & Pace, 1982). Hence, precipitation is achieved by decreasing its solubility using organic solvent such as ethanol and isopropyl alcohol (IPA) (Galindo & Albiter, 1996; Gonzales *et al.*, 1989). A ratio of 3:1 (organic solvent: broth volume) is needed to precipitate the xanthan gum when IPA or acetone is used and ≥ 6 volume is needed when lower alcohol such as ethanol is used (García-Ochoa *et al.*, 2000). On the other hand, when cell-free xanthan gum is required, cells separation is carried out by centrifugation of diluted fermentation broth. The cell separation by dilution process from highly viscous

xanthan solution is a cost-intensive process. Thus, adding alcohol and salt would aid the precipitation process (García-Ochoa *et al.*, 1997). The wet solid of xanthan obtained will then undergo repeated process of dewatering, washing, re-dissolving and precipitation to achieve the final purity required. Finally, the xanthan gum is spray dried and milled to the desired mesh size (Rosalam & England, 2006).

2.1.3 Xanthan gum molecular structure

Each repeating unit of xanthan gum comprises of cellulosic backbone of *β*-1,4 glycosidic linked glucose molecules with trisaccharide side chains. The side chains are *α-D*-mannopyranose unit attached by 3-1 linked to every second glucose unit of the main chain, 2-1 linked *β-D*-glucoronic acid and terminal 4-1 linked *β-D*-mannopyranosic unit. Acetate and pyruvate are attached to inner and terminal mannose respectively (Dário *et al.*, 2011). The chemical structure of xanthan gum is shown in Figure 2.1.

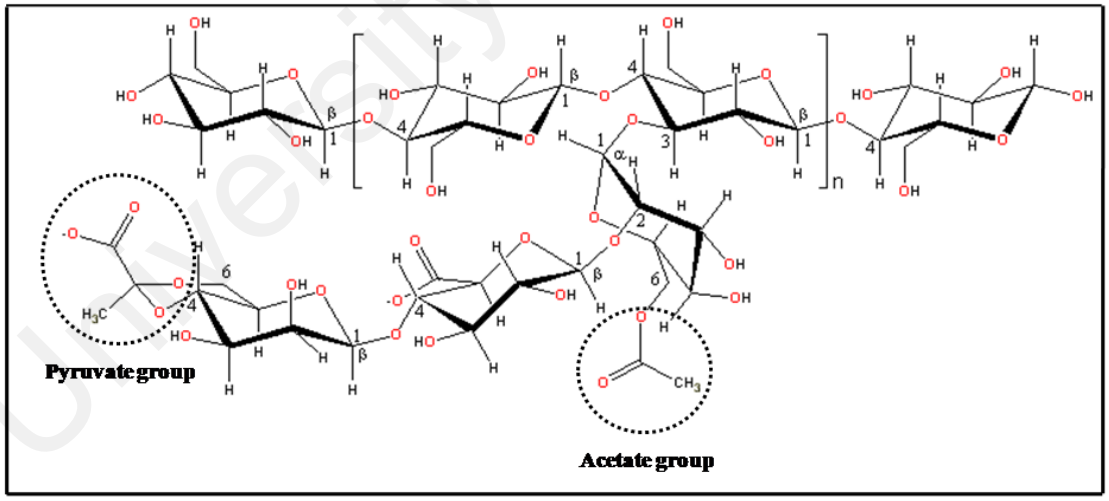

Figure 2.1 Structure of the repeating unit of xanthan gum

(Ciesielski & Tomasik, 2008)

2.1.3.1 Reducing ends

A free aldehyde/ ketone group bearing carbohydrate is able to act as reducing agent and hence called reducing sugar. This reducing property is obtained when a free anomeric carbon of a monosaccharide that is not involved in glycosidic bond is available (Wolfrom & BeMiller, 1963). Thus, the cyclic ring form of this monosaccharide is capable of opening and converted to an open chain form bearing the free aldehyde group, also called as reducing ends. One of the established methods in detecting reducing sugar is by using Dinitrosalicyclic acid (DNS) reagent. 3,5-Dinitrosalicylic acid molecule is an aromatic compound that reacts with reducing molecules to form 3-amino-5-nitrosalicyclic acid which strongly absorbs light. The formation of reducing ends, as a result from the breakage of glycosidic bonds would be prevalent in the degradation of xanthan gum, and therefore can be determined by using DNS method.

2.1.4 Xanthan gum order-disorder conformational transition

Many investigations have been carried out to study the conformational transition of xanthan gum. Xanthan gum is believed to exist in ordered and disordered conformational structure. This transitional between order-disorder is induced by manipulating the presence of salt in xanthan gum solution and exposure towards temperature. In the ordered conformation, the side chains are folded in and associated with the backbone, while in the disordered structure, the side chains are not associated and projected away from the backbone (Pelletier *et al.*, 2001). Different approaches that are employed to study this conformational transition behaviour are shear and extensional flow (Pelletier *et al.*, 2001), light scattering measurement (Capron *et al.*, 1997; Liu *et al.*, 1987; Sato *et al.*, 1984), atomic force microscopy (Camesano & Wilkinson, 2001), optical rotation, viscometry and potentiometric titration (Holzwarth,

1976), differential scanning calorimetry (Kitamura *et al.*, 1991), small angle neutron scattering (Milas *et al.*, 1995), and electron microscopy (Stokke *et al.*, 1987). It is important to understand xanthan gum transitional behaviour in solution as it could be manipulated to achieve a higher degree of degradation.

2.1.4.1 Native/ ordered conformation

The ordered conformation of xanthan gum is extensively investigated. In solution, the ordered xanthan gum molecules exist in a semi-rigid helix that is stabilized by hydrogen bonding between side chain and main chain, and can undergo a conformational transition to a disordered chain either by decreasing salinity or by increasing temperature to above its melting temperature (Capron *et al.*, 1997; Morris *et al.*, 1983). It is either this helical structure exists in a single helix or double helix form that sparks debate between researchers. However, it is concluded that the ordered conformation of xanthan gum is double stranded helix based on the result obtained using electron microscopy (Holzwarth & Prestridge, 1977). This statement is further supported by Paradossi and Brant (1982) that estimated the molar mass per unit contour length of xanthan to be 2000 nm^{-1}, a value twice for a single xanthan chain based on hydrodynamic and light scattering data. Sato *et al.* (1984) later concluded that xanthan gum has the fivefold double stranded helical structure with an intermediate rigidity between double stranded DNA and the triple helix schizophyllan, evidence obtained from using light scattering method.

2.1.4.2 Denatured/disordered conformation

Conformational transition from ordered to disordered molecule occurs when xanthan gum is exposed to decreasing salt concentration and increasing temperature. The denaturation temperature (T_m) was reported to occur at temperature near 50 °C in 0.01 M NaCl solution. The reduction in molecular weight of xanthan gum started to occur at 50 °C and eventually become half of its initial value at 60 °C. The molecular weight becomes half by means of the dissociation of the ordered double stranded into disordered single chain. Despite the reduction in molecular weight, it is interesting to note that reduction in molecular size and solution viscosity are not immediately evident during the denaturation temperature range. This indicates that xanthan gum undergoes intermediary state before completely denatured, during which the side chain that represents 65 % of the molecular weight play a major role on the disordered conformation (Capron *et al.*, 1997).

However, study carried out by (Matsuda *et al.*, 2009) shows that denaturation process of xanthan gum is also controlled by its concentration. In dilute solution of < 1.0 mg cm^{-3}, the xanthan dimer dissociates into two single chains in 80 °C water while at high concentration (10 mg cm^{-3}), the xanthan double helix unwound from both end portions but does not dissociate into two single chains. A study of xanthan gum denaturation in salt solution using high sensitivity differential scanning calorimetry shows that the temperature of conformation transition increase linearly with the logarithm of the cation (Na^+, K^+) concentration (Kitamura *et al.*, 1991). However, this transition temperature was found to be independent of the molecular weight of xanthan gum sample.

2.1.4.3 Renatured/ordered conformation

Denaturation process is reversible. The ordered conformation could be regained by quenching and adding salt to the temperature induced disordered xanthan gum solution. This process is called renaturation. Despite in the ordered state, renatured xanthan does not recover its full native form. According to Matsuda *et al.* (2009), the renatured xanthan gum exists in two different conditions depending on the xanthan gum solution concentration. In dilute xanthan gum solution (<1 mg cm^{-3}), the dissociates xanthan gum chains reconstruct the intra-molecular double helical structure with a hairpin loop while in concentrated xanthan gum solution (10 mg cm^{-3}), the xanthan dimer aggregates by mismatched pairing. The renaturation model is illustrated in Figure 2.2.

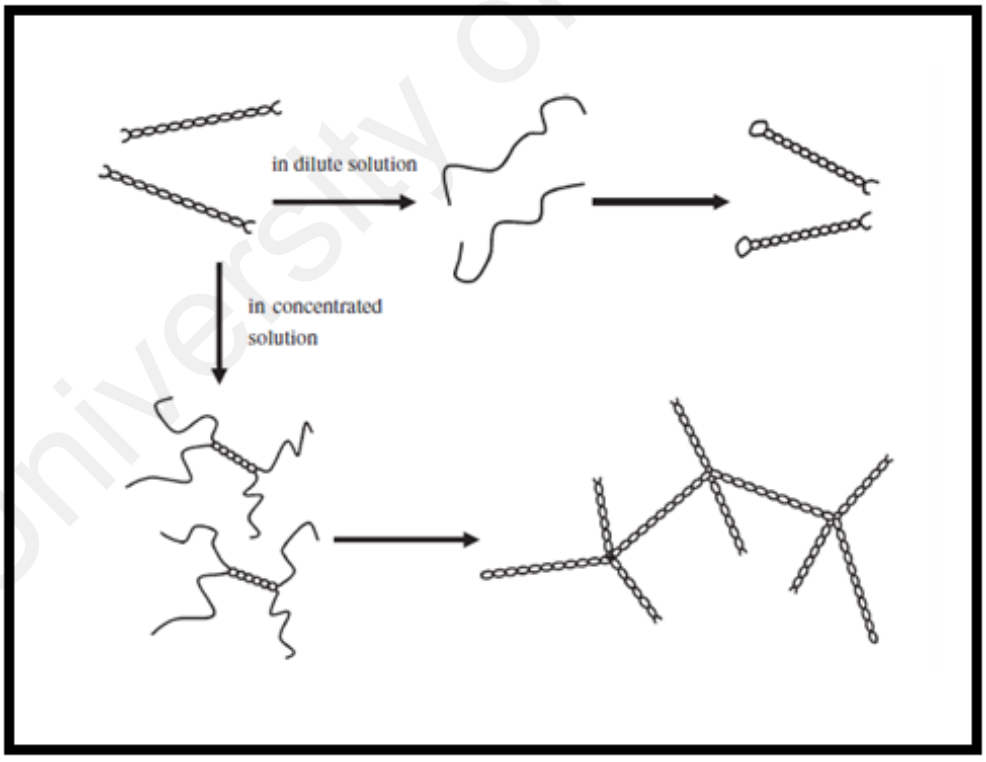

Figure 2.2 Renaturation model in different conditions of xanthan gum solution (Matsuda *et al.*, 2009)

The presence of ionic salts in xanthan gum solution plays a major role in the renaturation process. Incomplete renaturation occur as thin regions and loops representing the single helical structure observed under atomic force microscopy and this are abundantly found in pure water. These regions however are not observed when salt is present in the xanthan gum solution. The contour length and persistence length of the renatured xanthan gum also decreases at increasing salt concentration. Following temperature quenching, number and average contour length of xanthan gum in pure water is reported to be 1651 and 1922 nm respectively. This value decreases to 450 and 603 nm in 0.1 and 0.5 KCl respectively. In addition, less rigid xanthan gum molecules are observed at increasing salt solution. The persistence length, L_p in pure water is 417 nm and decreases to 370 when salt is present (0.01 M KCl) and further reduces to 140 - 170 nm in 0.1 M and 0.5 KCl. These decreasing values prove the reformation of double helical structure from single strand chain during renaturation and could only occur when salt is present (Camesano & Wilkinson, 2001). Aggregation process is also enhanced during renaturation process at increasing salt concentration. It is shown by the increases in apparent molecular weight of xanthan gum in renatured xanthan than in the native state (Ikeda *et al.*, 2012).

2.1.4.4 The importance of xanthan gum side chain

Acetate and pyruvate can be found on mannose residue that is attached to xanthan gum backbone and terminal mannose respectively. The variability of these units on every side chain of xanthan gum repeating unit depends on the fermentation conditions, strain of *Xanthomonas* and xanthan gum recovery procedure (Young *et al.*, 1994). These two molecules govern the xanthan gum conformational transition and the viscosity behaviour (Young *et al.*, 1994). Therefore, to take control of xanthan gum

properties, acetate and pyruvate can be selectively removed. Acetyl-free xanthan gum can be obtained by saponification treatment with 1M NaOH for 18 hour at 4 °C. On the other hand, to remove pyruvate from side chain, xanthan gum needs to be heated at 100 °C in a 5 mM trifluoroacetic acid (TFA) solution (Bradshaw *et al.*, 1983).

In order-diorder transition of xanthan gum, acetate group tend to stabilize the ordered conformation while disordered xanthan gum is favoured by pyruvate group. Stabilization of ordered conformation is through hydrogen bonding that occurs between methyl residues of acetate group and the adjacent oxygen atom of *D*-glucose at the main chain (Tako & Nakamura, 1989; Tako *et al.*, 2014). In contrast, the disordered conformation is favoured by pyruvate group because in this form, the side chain is extended away from the main chain of xanthan gum, hence the electrostatic repulsion between pyruvate group and the backbone is minimized (Kool *et al.*, 2013a). Therefore, de-pyruvated xanthan gum recorded a higher ordered-disordered transition temperature compared to native xanthan gum sample.

However, Kool *et al.* (2014) found that the distribution of acetate and pyruvate unit on xanthan gum side chain are completely random. Double acetylated xanthan gum repeating unit is found where the pyruvate unit on terminal mannose is replaced by an acetate group. This specially acetylated terminal mannose is responsible in stabilizing xanthan gum ordered conformation since acetylation of the inner mannose does not show clear stabilizing effect.

2.1.5 Properties of xanthan gum

Xanthan gum is a highly viscous polymer even at a low concentration. This viscosity properties that resist flow contributes to the thickening ability of xanthan gum. At increasing shear rate, the viscosity of xanthan gum decreases making it a pseudoplastic or shear-thinning polymer. The viscosity is also affected by temperature, polymer concentration, concentration of salts and pH. Due to the polyelectrolyte nature of xanthan gum, it is highly soluble in both cold and hot water (Katzbauer, 1998).

2.1.6 Applications of xanthan gum

2.1.6.1 Food applications

In food industries, adding xanthan gum improves texture, flavour released, appearance, water-control properties and the rheology of the final food products. It also gives out less "gummy" mouth feel compared to gums with more Newtonian characteristics. Xanthan gum is used as suspending and thickening agent for fruit pulp and chocolates, increase water binding during baking, extending the shelf life of baked goods and refrigerated dough, maintaining the suspension of fruit pulps particles in beverages, stabilizing ice cream, sherbet and milk shakes by heat shock protection and ice crystal control. Salad dressings with xanthan gum have excellent long term emulsion stability. Added to its constant viscosity over a wide range of temperature range, dressings containing xanthan gum can be poured easily but at the same time cling well to the salad. In addition, xanthan gum aids in homogenizing gelled food products and making syrups and toppings of high consistency, appeared thick and appetizing (Palaniraj & Jayaraman, 2011; Rosalam & England, 2006; Saha & Bhattacharya, 2010; Sanderson, 1981)

2.1.6.2 Industrial applications

Other than extensive applications in food products, xanthan gum is also widely beneficial in other fields. The rheological properties of xanthan gum allow it to be used in petroleum industry. Xanthan gum is utilized in oil drilling, fracturing and pipeline cleaning. Due to its high resistance to thermal degradation and compatibility with salts, xanthan gum is added in drilling fluids as an additive (Sandvik & Maerker, 1977). Xanthan gum is also extensively used as viscosifier in oil industry and aid in the fluid loss control during drilling, stimulation treatments, and hydraulic fracturing (Navarrete *et al.*, 2000).

In the agricultural industry, xanthan gum increases the contact time between the pesticide and crop due to improved flow-ability formulations of fungicides, herbicides and insecticides.

Stable over broad pH range, xanthan gum is the preferred choice in highly alkaline and acidic cleaning solutions. For example graffiti remover, toilet bowl cleaner and aerosol oven cleaner. Addition of xanthan gum in such products provides cling to vertical surface and allows the cleaning solution to be easily removed.

Xanthan gum thickens latex paints and coatings, and uniformly suspends zinc, copper and other metal additives in corrosion coatings.

In personal care products namely shampoos and liquid soaps, adding xanthan improves its flow properties and promotes a stable, rich and creamy lather. Besides that, xanthan gum is an excellent binder for all toothpastes and eases the extrusion process.

The suspensions of insoluble materials in pharmaceutical products e.g. complexed dextromethorphan for cough medication are also stabilized with the addition of xanthan gum (Palaniraj & Jayaraman, 2011; Rosalam & England, 2006; Sandvik & Maerker, 1977).

2.2 ULTRASONIC DEGRADATION

2.2.1 Ultrasonic probe system

Sonication using ultrasonic probe surpass the ultrasonic bath in sonochemistry by means of high power supply and control of the energy input to the chemical reaction. By using ultrasonic probe, the vibrating transducer is immersed directly into the reaction solution. Hence, increasing the amount of ultrasonic power transmission into the solution due to direct supplied energy.

In ultrasonic probe system, a sonic horn is attached to the end of the transducer. This metal rod extension helps in magnifying the amount of power (amplitude of vibration) supplied and keeping the transducer clear from the chemical reaction since only the tip of the rod needs to be immersed in the liquid. The overall ultrasonic probe system consists of generator, transducer and a horn as shown in Figure 2.3. The alternating electrical current is transformed into 20 kHz in generator that is equipped with power control to control the amount of power supplied to transducer. To prevent excessive generation of heat during sonication, the power supplied to the probe can be put on switched 'on' and 'off' mode repeatedly. Therefore, during this 'off' time, the system is allowed to cool down in between the pulses. The piezoelectric transducer then converts this electrical signal into mechanical vibration. This vibration is amplified and transmitted down the length of the horn where the tip is expanded and contract longitudinally (Faïd *et al.*, 1998).

The horn comes in many shapes and length. In this study, a stepped horn is used. The material used to build a horn is critically important, as it should resist the cavitation erosion, chemically inert and provide low acoustic loss. Therefore, to fulfil this purpose, the best material to build up a horn is titanium alloy (Mason & Peters, 2002).

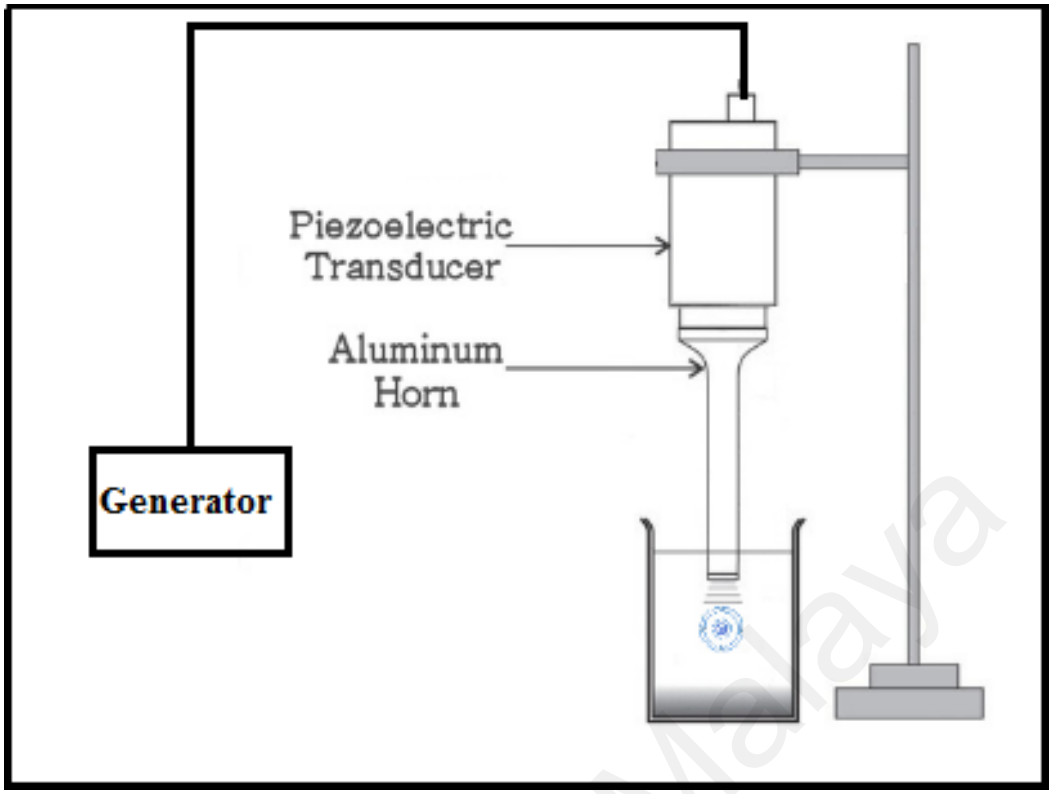

Figure 2.3 Schematic of ultrasonic probe system

2.2.2 Principle of ultrasonic degradation

The principle of ultrasonic processing relies on the behaviour of a sound wave. Ultrasound can be categorized into three categories depending on the range of frequency used. Power ultrasound (20 - 100 kHz) is used for industrial processing and sonochemistry, high frequency ultrasound (100 kHz - 1 MHz) is used for animal communication, detection of cracks in solid and under water echo-location and frequency range of 5 - 10 MHz ultrasound is used for diagnostic purposes (Martini, 2013).

When ultrasound is introduced into a reaction system, the sound wave is transmitted through vibration of the molecules medium. Propagation of the sound energy is through oscillation of the molecules. Each of the molecules transmits the vibration motion to adjoining molecule before returning to its approximately original position. In liquid and gas medium, oscillation of the molecules takes place in the same

direction of the wave hence producing longitudinal wave while in solid medium, the particles move in perpendicular direction of the wave thus producing transverse wave (Lorimer & Mason, 2002). Oscillation of these medium particles is powered by a cyclic succession of rarefaction and compression phase (Figure 2.4). Particles of the liquids are pushed towards each other during compression cycle by exerted positive pressure and pulled apart during rarefaction cycle due to the exerted negative pressure of the ultrasonic wave. When the negative pressure exceeds the tensile strength of the liquid during the rarefaction phase, the liquid is torn apart thus small vapour filled voids called cavitation bubbles are formed. This is what we called as cavitation threshold. These cavitation bubbles eventually grow in size during these successive cycles and become unstable. When the microbubbles can no longer absorb energy efficiently, the surrounding liquid will rush in and causing implosion during the compression cycle of ultrasonic wave. During the cavitation process, the size of the bubbles would increase drastically from tens to hundreds times its size and violently collapse in less than a microsecond (Figure 2.5). Therefore cavitation is the process of microbubbles nucleation, bubble growth and implosion. These collapsing actions of microbubbles or cavitation process as a whole are responsible for the all the reaction that takes place in ultrasonic processing (Pilli *et al.*, 2011; Suslick, 1994; Suslick & Price, 1999)

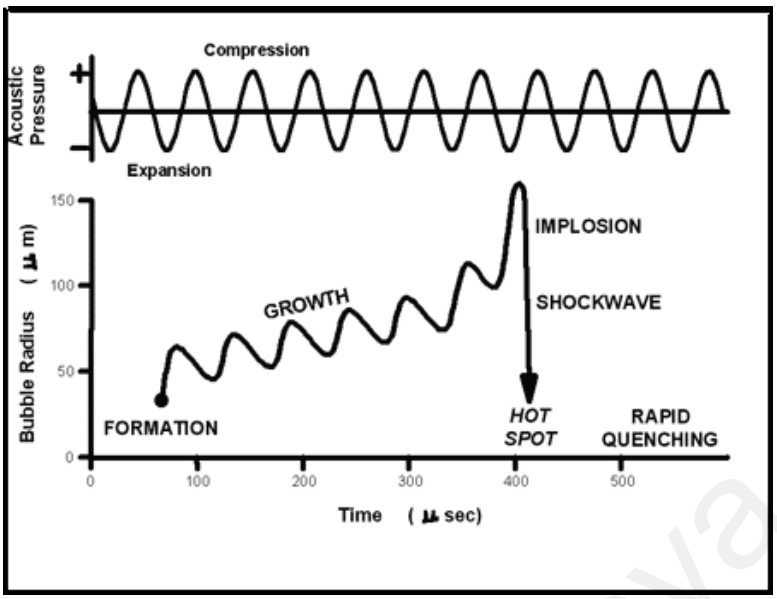

Figure 2.4 Cavitational process

(Suslick, 1994)

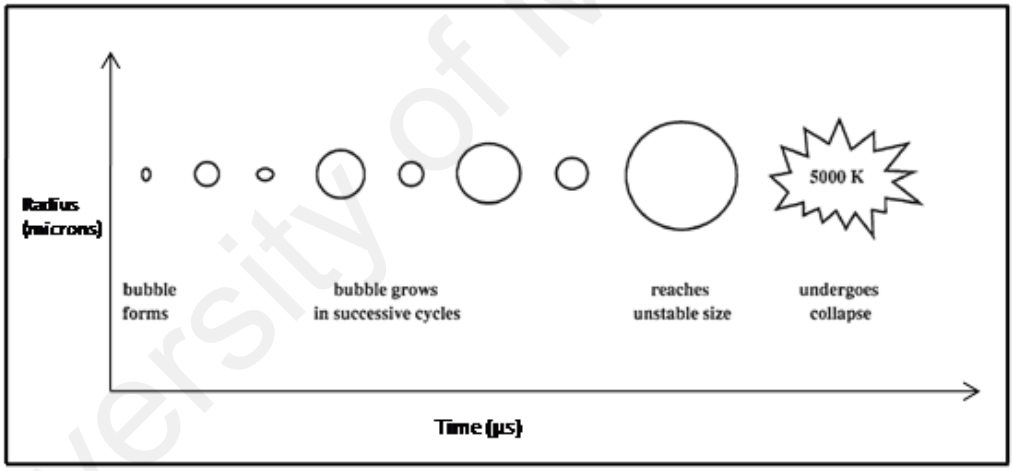

Figure 2.5 Development and collapse of microbubbles

(Pilli *et al.*, 2011)

2.2.3 Factors involve in cavitation

2.2.3.1 Gas

It is estimated that the acoustic pressure required in initiating the cavitation in water is approximately 1500 atm. However, from studies that have been conducted, this required value is a lot lower i.e < 20 atm (Lorimer & Mason, 2002). Cavitation as discussed previously is initiated when the critical molecular distance to hold the liquid intact is exceeded due to the sufficiently large negative pressure being imposed. The need for a lower acoustic pressure value in cavitation is directly attributed to the actual lower liquid's tensile strength due to the presence of weak spots. One cause of the formation of weak spots is the presence of gas molecules in the liquid. Therefore, degassing was found to have increased the cavitation threshold. Similar result obtained when external pressure is applied that will dissolve the suspended gas molecules. Increasing the cavitation threshold as a result of elimination of these gas nuclei eventually lead to an increase of negative acoustic pressure needed to apply to overcome the liquid tensile strength. This process eventually leads to the requirement of higher intensity sound wave. Therefore, to achieve a higher degradation, an opposite action must be performed i.e by saturating the liquid with gas to achieve a lower cavitational threshold. Threshold is lowered due to increased in gas nuclei (weak spots) in the liquid. Lowered cavitational threshold that lead to an easier cavitational process will release a significant force on the liquid system when the microbubbles collapsed during compression cycle (Mason & Peters, 2002).

2.2.3.2 Frequency

At higher frequency, a cycle of rarefaction and compression need to be completed in a shorter time. Therefore, the difference in the frequency applied would give an effect in the time of cavitation process. The cavitation process that starts with formation of void after complete rupture of the liquid, followed by the filling of gas or vapour in the cavity and increases of the size until reaching the maximum negative pressure becomes harder to achieve in this shorter available time. Therefore, to ensure this cohesive force of the liquid is overcome, a greater sound intensity will need to be employed over this shorter period. As the frequency increases, bubble formations are more limited. Ten times more power is required to initiate cavitation at 400 kHz than 10 kHz and it is reported that cavitation does not occur at frequencies above 2.5 MHz. Due to the difference in achievable result at different frequencies, frequencies of 20 - 50 kHz is generally chosen in the sonochemical applications since lower frequency clearly provides sufficient time for the microbubbles to fully expand, hence releasing higher energy when imploding. Frequency of below 16 kHz is also not suitable to be used because it will lead to noise discomfort since it is within audible range (Asgharzadehahmadi *et al.*, 2016).

2.2.3.3 Solvent

Proper selection of solvent for sonication is very crucial in order to optimize polymer degradation. There are few properties of solvent that involved in the increment of degradation rate. The major effect is solvent vapour pressure. As the solvent vapour pressure increases, the amount of polymer degradation decreases (Mason & Lorimer, 2003a). High vapour pressure has low enthalpy of vaporization (ΔH_v) making the solvent more volatile and hence easier to penetrate into the microbubbles. Upon collapsing of the microbubbles, the molecules of the solvent will give a cushioning

effect by slowing down the movement of the solvent, hence the less shock wave impact. In addition, the type of the solvent used is equally important. Imploding cavitational bubbles release energy more effectively in "good solvents" rather than in "poor solvents". It was found that adding "non solvent" acetone to solutions of polystyrene in benzene decreases the degradation rate (Lorimer & Mason, 2002).

2.2.3.4 Experimental temperature

Increasing the reaction temperature allows cavitation to be achieved at lower acoustic intensity due to the rise in liquid vapour pressure (P_v) or lower surface tension (σ). Despite the easily formed microbubbles at higher temperature, the consequence of its high vapour pressure as mentioned previously will reduce the effect of microbbubles implosion, which is responsible in releasing high energy shear force, hence reducing the degradation significance. Increasing the reaction temperature also decreases the viscosity of the solvents and polymer solution. Reduced viscosity however is beneficial to degradation since cavitation is easier to be achieved (Mason & Peters, 2002).

2.2.3.5 Sonication intensity

The intensity of ultrasound plays an important role in creating cavitation in a liquid. Cavitation can only occur when the liquid cavitation threshold is overcome by supplying sufficient ultrasonic intensity. Increasing the intensity will increase the sonochemical effect by the increase in size of microbbubles. However, intensity cannot be increased indefinitely since maximum size bubble is dependent upon pressure amplitude. Increase in pressure amplitude (P_A) causes the bubble grow so large during rarefaction cycle that the time available for collapse is insufficient (Asgharzadehahmadi *et al.*, 2016)

2.2.3.6 Concentration of solution

Several researchers have studied the effect of polymer concentration on degradation. Based on the results, the increase in polymer concentration has been found to reduce the degradation rate. The increase in concentration solution is closely related to the increase in solution viscosity. As the viscosity of the liquid increases, the natural cohesive force of the liquid becomes higher hence increasing the cavitation threshold of the liquid simultaneously. Therefore, cavitation is harder to be achieved in viscous solution making less impact upon collapsing (Lorimer & Mason, 2002).

In conclusion, manipulation of aforementioned sonication paramaters aids in the cavitation process hence enhancing the effect of ultrasonic processing. Some of the paramaters affecting xanthan gum degradation have been studied namely:

a) Saturating the polymer solution with gas;

b) Using a solvent with a low vapour pressure;

c) Reducing the experimental temperature;

d) Reducing the ultrasonic frequency;

e) Increasing the intensity of irradiation and

f) Decreasing the solution concentration.

2.2.4 Mechanism of ultrasonic degradation on polymer

Broad applications of ultrasound are seen in different areas namely cleaning and decontamination, cell disruption, dentistry and medicine, synthesis and degradation and many more. The powerful impact of cavitation is the key to this broad utilization. Upon collapsing, each of the bubble would act as a hotspot, generating energy to increase the temperature and pressure up to 5,000 K and 500 atm respectively and cooling rate as fast as 10^9 Ks^{-1}. The high local temperature and pressure will provide means for driving high-energy chemical reactions.

According to hot spot theory, each microbbuble acts as a small micro-reactor, which produces different radical species and heat during its collapse. Sonolysis of water when exposed to ultrasound produce radicals species such as hydrogen, (H^+), hydroxyl, (OH^-), and hydrogen peroxide, (H_2O_2). The reactive radicals readily react with other dissolved species.

Besides chemical reaction, ultrasound can also impose physical effects. Effects such as micro-streaming, micro-turbulence, micro-jets and shock waves can also be produced by cavitation bubbles resulting from the turbulent fluid movement and a micro-scale velocity gradient in the vicinity of cavitational bubbles (Moholkar *et al.*, 2015). These massive chemicals and physical effects imposed by collapsing bubbles are responsible in the degradation of polymer when exposed to high intensity ultrasound.

Define as lowering of the chain length caused by the cleaving action, degradation does not necessarily lead to a chemical change. Ultrasonic degradation of polymer is seen to occur rapidly at high molecular weight and approaches a limiting molecular weight below which no further degradation takes place. The behaviour is as result of a physical process that is independent of the chemical nature but rather depends on the polymer chain dimension.

The cleaving action by ultrasound occurs at specific section i.e near the middle of polymer chain length compared to thermal degradation that takes place more randomly along the chain. Degradation of the polymer through chemical reaction by generated radical species however, is only prominent at higher frequencies range (200 - 600 kHz) (Koda *et al.,* 2011). Therefore, the resulting bond breakage of xanthan gum when exposed to ultrasonic irradiation of power ultrasound used in this study is primarily attributed to the mechanical means, i.e shock waves produced after bubbles implosion and immediate exposure to the large force in the liquid flows in the vicinity of collapsing bubbles (Kasaai, 2013; Mason & Lorimer, 2003b).

2.2.5 Advantages of ultrasonic degradation

Along with the current rapid industrial development, continual improvement on existing material has become of great significance. Modification of polymers will produce highly functional materials hence adding more values to them. One of the many methods of polymer modification being utilized is controlled degradation. Similarly, the high molecular weight and particle size of xanthan gum need to be reduced by means of controlled degradation in order to expand its functionalities. The different modes of xanthan gum degradation to its dimension of preference have been studied by different researchers i.e chemical degradation (Christensen *et al.*, 1996; Christensen & Smidsrød, 1991; Christensen *et al.*, 1993; Stokke & Christensen, 1996), enzymatic degradation (Cheetham & Mashimba, 1991; Kool *et al.*, 2014; Kool *et al.*, 2013b), thermal degradation (Lambert & Rinaudo, 1985) and ultrasound-mediated degradation (Li & Feke, 2015; Milas *et al.*, 1986; Tiwari *et al.*, 2010). Chemical and enzymatic methods have drawbacks such as higher treatment time and costs are needed. Uniform molecular weight distribution is also hard to be achieved when using these methods of degradation (Prajapat & Gogate, 2015). Using chemical treatment e.g. hydrogen peroxide has low

product yield and polluting the environment as chemical waste is produced (Czechowska-Biskup *et al.*, 2005; Liu *et al.*, 2006). Ultrasonic degradation on the other hand is considered as greener, simpler, rapid, energy saving, effective and by-product free compared to other degradation methods (Huang *et al.*, 2015; Liu *et al.*, 2006; Wu *et al.*, 2008). In ultrasonic degradation, a large batch of samples can be irradiated at one particular time hence decreasing the overall reaction time needed (Tsaih & Chen, 2003). Ultrasound does not change the chemical nature of the polymer as it effectively split the most liable chemical bond whereas other methods might alter the chemical structure and hence the material behaviour (Grönroos *et al.*, 2001; Li & Feke, 2015; Prajapat & Gogate, 2015).

2.3 Functions of degraded xanthan gum

2.3.1 Crop protecton strategy

Degraded xanthan gums promised many significant potentialities. Xantho-oligosaccharides produced by Qian *et al.* (2006) through enzymatic hydrolysis has been shown to inhibit the growth of *Xanthomonas campestris pv. campestris.* In addition, the virulence factor of this pathogenic bacteria i.e the production of xanthan gum has also been reduced. The anti-bacterial activities of xantho-oligosaccharides are widened due to their additional capabilities in partially inhibiting the production of extracellular enzymes released from *X. Campestris pv. campestris viz.* cellulase, chitinase, pectinase and proteinase.

A study carried out by Liu *et al.* (2005) showed xantho-oligosaccharides produced by degradation of xanthan gum from *Cellulomonas* sp. as active elicitors. Elicitors are inducer to promote the synthesis of phytoalexins, a low molecular weight antimicrobial product of higher plants. It is found that that the xanthan-degraded products are able to induce the phytoalexin accumulation in soybean cotyledon tissues. Thus, xantho-oligosaccaharides, a degraded xanthan gum product is proved to be beneficial in the applications of plant protection strategy, which is a good alternative to the harmful application of pesticides.

2.3.2 Antioxidants

Xanthan gum degradation also promotes the production of xanthan oligosaccharides with good water solubility and bioactivity. The other recorded bioactivity of xanthan oligosaccharides is its antioxidant properties. Different antioxidant properties produced are ascribed to the different degradation treatments, which lead to the different structures of xanthan oligosaccharides with respect to its pyruvate content and reducing sugars. Xantho-oligosaccharides are found to exhibit

good antioxidant activities towards superoxide anion radical, hydroxyl radical, 2,2-diphenyl-1-picrylhydrazyl (DPPH), hydrogen peroxide and ferrous ions (Xiong *et al.*, 2013). The incorporation of xanthan gum fragments obtained by degradation using hydrogen peroxide in the presence of ferrous ions (Fenton system) into semi-solid formulation for topical administration captured the attention of Trommer and Neubert (2005) since its addition showed effective protection of α-linolenic acid (LLA) from UV-induced damage.

CHAPTER 3

MATERIALS & METHODS

3.1 MATERIALS

Xanthan gum powder was purchased from R&M Chemicals, sodium chloride (NaCl), glucose, and 95 % (w/w) sulphuric acid (H_2SO_4) were purchased from Merck. Dinitrosalicyclic acid (DNS) was purchased from Sigma, sodium hydroxide (KOH) and potassium sodium tartarate (Rochelle salt) were purchased from Systerm, phenol was purchased from Hamburg Chemicals, sodium sulphite and barium carbonate ($BaCO_3$) were purchased from BDH Chemicals. All chemicals were of analytical grade.

3.2 PREPARATION OF XANTHAN GUM SOLUTION

Xanthan gum solutions were prepared by dispersing dried xanthan gum powder in deionized water at pre-determined concentrations. Solutions were stirred to obtain full hydration. The influence of ionic strength on ultrasonic degradation was studied by pre-mixing the solution with NaCl before sonication.

3.3 SONICATION SYSTEM SETUP

Sonication treatment was carried out using a probe ultrasonic sonifier (Branson Digital Sonifier (Model 450) USA) that comprised of 102–C converter, standard disruptor horn, and digital power control unit. The sonifier has a maximum power output of 400 W, operated at a frequency of 20 kHz. The power supplied to the solution and total duration of irradiation was set by adjusting power percentage (%) displayed on the control unit component. Sonication was carried out by immersing the disruptor horn into the aqueous solution of xanthan gum (30 mL) placed in a cylindrical borosilicate glass vessel. The disruptor horn was centrally fixed to immerse into half of the solution

height for even power transfer. The solution was irradiated with acoustic wave for a specified duration at 2s 'ON' and 1s 'OFF' cycle. The schematic and specification of sonication system setup were shown in Figure 3.1. To control the temperature increase during sonication, the glass vessel was placed in cooling compartment connected to a cooling bath (WCR – P8, Daihan Scientific Co. Ltd) operated at 10 °C. During sonication, the temperature of the sample solution was measured to be in the range of 35 – 40 °C.

3.4 DETERMINATION OF ACOUSTIC POWER DISSIPATION

Due to power losses during acoustic transfer into the samples, assessment on the measured acoustic power dissipation in the samples was carried out. Three different sizes of cylindrical vessels were tested to determine the dissipated acoustic power. The specifications of the different vessels were shown in Table 3.1. The acoustic power entering the liquid was set to be at 60 %.

Table 3.1. Specifications of the three sonication setups

Vessel volume	**Vessel base diameter, *D* (cm)**	**Vessel base area, *A* (cm^2)**	**Vessel height, *H'* (cm)**	**Liquid height, *H* (cm)**	**Liquid volume, *V* (cm^3)**	**Distance of the horn tip, *T* (cm)**
A (50 ml)	4.0	12.6	5.5	2.6	32.7	1.3
B (100 ml)	4.6	16.6	7.0	2.0	33.2	1.0
C (150 ml)	5.4	22.9	8.4	1.6	36.7	0.8

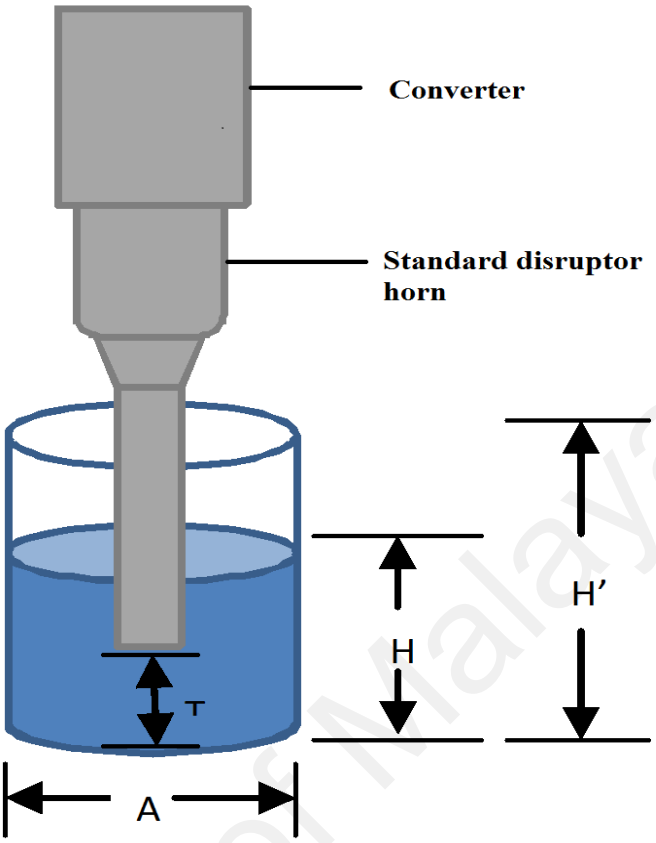

Figure 3.1 Schematic design of sonication sytem setup where *H*' is the height of glass vessel, *H* is the liquid height of the sample, *T* is the distance of the horn tip from vessel base and *A* is the area of the vessel base

3.5 CALCULATIONS

The actual power (Watt) dissipated in the sample was measured calorimetrically by measuring the time-dependent change of the solution temperature following Equation 3.1. (Mason *et al.*, 1994):

$$P = \frac{\Delta T}{\Delta t} \times C_p \times m \qquad (3.1)$$

where,

P = Power (W),

m = Mass of the xanthan gum solution (g)

C_p = Specific heat capacity of water (4.18 J g^{-1} K^{-1})

($\Delta T/\Delta t$) = slope of changes in temperature (K) over irradiation time t (s).

Ultrasonic intensity, I was calculated according to Equation (3.2):

$$I = \frac{P}{A} \qquad (3.2)$$

where,

P= Power (Watt)

A= Probe tip surface area (cm^2).

Ionic strength, I of the NaCl solution was calculated according to Equation (3.3):

$$I = \frac{1}{2}\sum M_i Z_i^2 \qquad (3.3)$$

where,

M_i = molarity of ion

Z_i = net charge of ion.

3.6 SCREENING OF SELECTED SONICATION PARAMETERS

Screening of four different sonication parameters were performed using Full Factorial Design (FFD) as designed in Minitab® 16 statistical software. The screened parameters were sonication intensity (Wcm^{-2}), irradiation time (minutes), concentration of xanthan gum ($g\ L^{-1}$) and concentration of NaCl (M) at lowest and highest factor levels as described in Table 3.2. The experiment was conducted in random triplicate resulting in 48 experimental runs. The design was completely randomized along with the sampling.

Table 3.2. Selected sonication factors for screening experiments

Factor	Low level	High level
Sonication intensity (Wcm^{-2})	2.7	11.5
Irradiation time (minutes)	30	120
Concentration of xanthan gum ($g\ L^{-1}$)	1	5
Concentration of NaCl (M)	0	0.1

The degree of xanthan gum degradation (%) was evaluated as the response using the calculation as shown in Equation 3.4.

$$Degree\ of\ degradation = \left(\frac{(OH)_f - (OH)_i}{(OH)_{theoretical} - (OH)_i}\right) \times 100 \qquad (3.4)$$

where

$(OH)_i$ = Initial moles of reducing ends present in the sample prior to sonication

$(OH)_f$ = Final moles of generated reducing ends following sonication

$(OH)_{theoretical}$ = The available mole of reducing ends generated following chemical hydrolysis of glycosidic bonds present in xanthan gum

3.7 REDUCING ENDS QUANTIFICATION

3.7.1 Dinitrosalicyclic acid assay

After each sonication run, the reducing ends generated from the sonicated samples were determined using DNS assay conducted in triplicate. 3.0 mL of sample was placed in a test tube. 3.0 mL of DNS reagent was then added into the sample and mixed followed by incubation in 90 °C water bath for 10 min. The DNS reagent was prepared by mixing dinitrosalicyclic acid, sodium hydroxide, phenol and sodium sulphite into deionised water. The reaction was stopped by adding 1.0 mL of 40 % (w/v) Rochelle salt into the mixture, and then let cooled at room temperature. The optical density (OD) of the treated solution was measured using spectrophotometer (2100 spectrophotometer, Cole Parmer) at 575 nm using DNS reagent added into deionised water as blank sample. The concentration of reducing ends yielded was calculated using standard calibration of glucose concentration (0 – 0.5 g L^{-1}).

3.7.2 Chemical hydrolysis

The theoretical available reducing ends of xanthan gum were determined by chemically hydrolyzing the glycosidic bonds present in xanthan gum sample. Xanthan gum hydrolysis was carried out following (Saeman *et al.*, 1954). Approximately 1.0 mL of 72 % (w/w) H_2SO_4 was added to 100 mg xanthan gum dry powder and mixed completely. The mixture was allowed to stand for 1 hour in 30 °C water bath. Hydrolysate was diluted by adding 29 mL deionised water preceding secondary hydrolysis performed at 120 °C for 90 min. Hydrolysate was then neutralized by adding $BaCO_3$. Neutralized hydrolysate was separated by adding 5.0 mL of deionised water followed by filtration using Whatman filter paper (No.1) placed in a filter funnel. The hydrolysate was then subjected to DNS assay to quantify the available reducing ends.

3.8 OPTIMIZATION OF SONICATION PARAMETERS

Optimization was carried out using a conventional one-factor-at-a-time (OFAT) method following screening of the selected sonication parameters. From the screening results obtained by Full Factorial Design, concentration ranges of NaCl and xanthan gum were further investigated to determine their optimum levels for efficient degradation of xanthan gum solution. The optimization was first studied by varying the xanthan gum concentration at (g L^{-1}) 0.1, 0.5, 5.0, 1.0, and subsequently the NaCl concentration at (M) 0, 1.0×10^{-4}, 1.0×10^{-3}, 1.0×10^{-2}, 1.0×10^{-1}. Irradiation time and intensity were fixed at 120 min and 11.5 Wcm^{-2}, respectively.

3.9 MEASUREMENT OF XANTHAN GUM SOLUTION VISCOSITY

The viscosity measurements of the xanthan gum at (g L^{-1}) 5, 1, 0.5 and 0.1 were carried out using a vibrating plate viscometer (Vibro Viscometer, SV-10, A&D Company, Japan), at 25 ± 1 °C. The titanium sensor plate of the viscometer was dipped into the xanthan gum solution and the viscosity reading was taken only after constant viscosity reading was achieved. The experiment was conducted in triplicate.

3.10 ANALYTICAL METHODS

3.10.1 Molecular Weight Analysis

Molecular weight analysis of sonicated and unsonicated xanthan polymer as control was carried out using size exclusion chromatography (SEC) that was performed on Agilent LC1220 (USA) equipped with binary pump (PU 980), auto sampler (AS 950), column oven (CO 965) and refractive index detector (RID) (Agilent). 0.1 g L^{-1} of sonicated and control samples were filtered through 0.2 µm PES filter and placed in clear vials. For 1 g L^{-1} sonicated xanthan sample, the aqueous sample was freeze dried and re-dissolved in deionised water to a final concentration of 0.1 g L^{-1} before injection

into the SEC system. The different molecular weight molecules were separated using separation column designated as WATERS Ultrahydrogel, Linear, 10µm, 7.8 mm × 300mm, 500-10M. Injection volume of 5 µL was used. The temperatures of the column and detector were kept constant at 30 °C. Elution was carried out using 100 % milliQ water as the mobile phase at a flow rate of 0.5 mL min^{-1}. The molecular masses obtained were calibrated against pullulan molecular-mass standards (Waters Corp.). The range of pullulan molecular-mass standards used were 5.9×10^3, 9.6×10^3, 21.1×10^3, 47.1×10^3, 107.0×10^3, 200.0×10^3, 344.0×10^3 and 708.0×10^3 Da.

3.10.2 Determination of thermal properties

Thermal behaviour of ultrasound-irradiated xanthan gum was investigated using Thermogravimetric Analysis (TGA) and Differential Scanning Calorimetry (DSC). TGA analysis was performed using Perkin-Elmer (USA), heated from 30 – 800 °C at a rate of 10 °C min^{-1} under a nitrogen gas flow rate of 20 mL min^{-1}. This analysis was used to determine the initial degradation temperature (T_d) of the polymer to support the chain scission model proposed. DSC analysis was carried out using TA Instrument (DSC Q10) at a temperature range of 30 to 300 °C and heating rate of 10 °C min^{-1} under nitrogen gas flow to study the behaviour of xanthan gum in salt solution upon exposure to ultrasonic irradiation.

3.10.3 Fourier-Transform Infrared Spectroscopy (FTIR)

Fourier-Transform Infrared Spectroscopy analysis was performed using Spectrum 400 (Perkin Elmer) spectrometer. Dried sonicated xanthan gum sample was casted on the NaCl FTIR cells as thin film. The spectra were recorded between 4000 and 500 cm^{-1}, with 4 cm^{-1} resolution and 10 scans at room temperature (25 ± 1 °C). The spectrum of the sonicated xanthan gum was then compared with the control sample.

3.10.4 Proton nuclear magnetic resonance analysis (^{1}H NMR)

^{1}H NMR spectra of xanthan gum samples were analysed using Bruker FT-NMR at 400 MHz. Approximately 6.5 mg of xanthan gum samples were dissolved in 1 ml of deuterated water (D_2O) and centrifuged at 8000 rpm for 3 min to remove air bubbles. Analysis was performed at 85 °C.

CHAPTER 4

RESULTS AND DISCUSSION

4.1 DETERMINATION OF ACOUSTIC POWER DISSIPATION

To maximise the ultrasonic power transmission into reaction solution, three different sonication setups were studied by utilizing three different sizes of cylindrical glass vessels that contained 30 mL xanthan gum aqueous solution (Figure 4.1). Sonication power output for irradiation was set at 60 % and the actual power dissipation was determined calorimetrically, and subsequently sonication intensity was calculated. Since power dissipation is a direct function of temperature change (Equation 3.1), its time profile can be used as an indirect measure of power dissipation inside the xanthan gum solution for all vessels studied (Figure 4.1). It was found that glass vessel *C* showed the lowest ultrasound irradiation power dissipation among the three setups tested i.e. at 37.4 ± 0.76 W. This was attributed to the highest area/volume where ultrasound power was dissipated for the configuration (*C*) (Table 4.1 and Figure 4.1). Significant difference in power dissipation was observed between vessel *C* and vessels *A*/*B* ($p < 0.05$). However, there was no significant difference in power dissemination between vessel *A* and *B* ($p > 0.05$), as shown in Figure 4.1. Consequently, vessel *B* (100 ml) was used throughout the study thereafter.

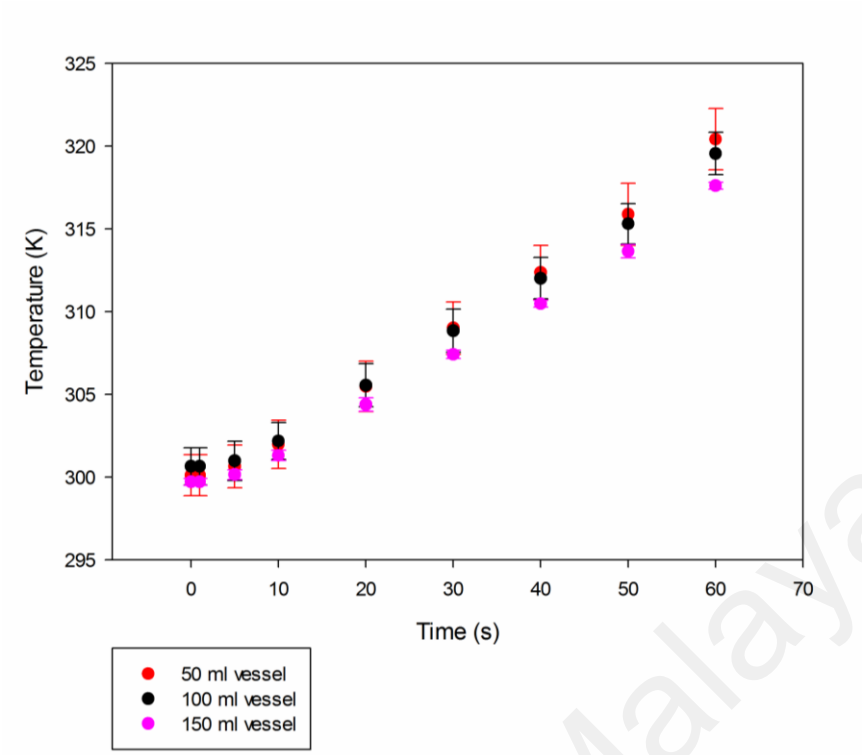

Figure 4.1Temperature changes as a function of temperature during calorimetric determination of ultrasound power dissipation in cylindrical glass vessels with different dimensions

Table 4.1 Power (W) and irradiation intensity (W cm^{-2}) in different sonication vessels

Vessel volume	**Actual power delivered (Watt)**	**Intensity (W cm^{-2})**	**Power dissipation per area (W cm^{-2})**	**Power dissipation per volume (W cm^{-3})**
A (50 ml)	42.5 ± 1.36	12.3 ± 0.40	3.37 ± 0.11	1.30 ± 0.04
B (100 ml)	39.6 ± 0.71	11.5 ± 0.21	2.39 ± 0.04	1.19 ± 0.02
C (150 ml)	37.4 ± 0.76	10.8 ± 0.22	1.63 ± 0.03	1.02 ± 0.02

4.2 REDUCING ENDS QUANTIFICATION

Theoretically, every fragments of xanthan chain that is no longer attach to the glycosidic bond following bond breaking will expose new reducing ends (Einbu & Vårum, 2003). The concentrations of reducing ends obtained following ultrasonic irradiation were quantified based on the glucose standard calibration (Figure 4.2). Assayed using DNS, the values were used as the response in both screening and optimization of sonication operating variables following Equation (3.4).

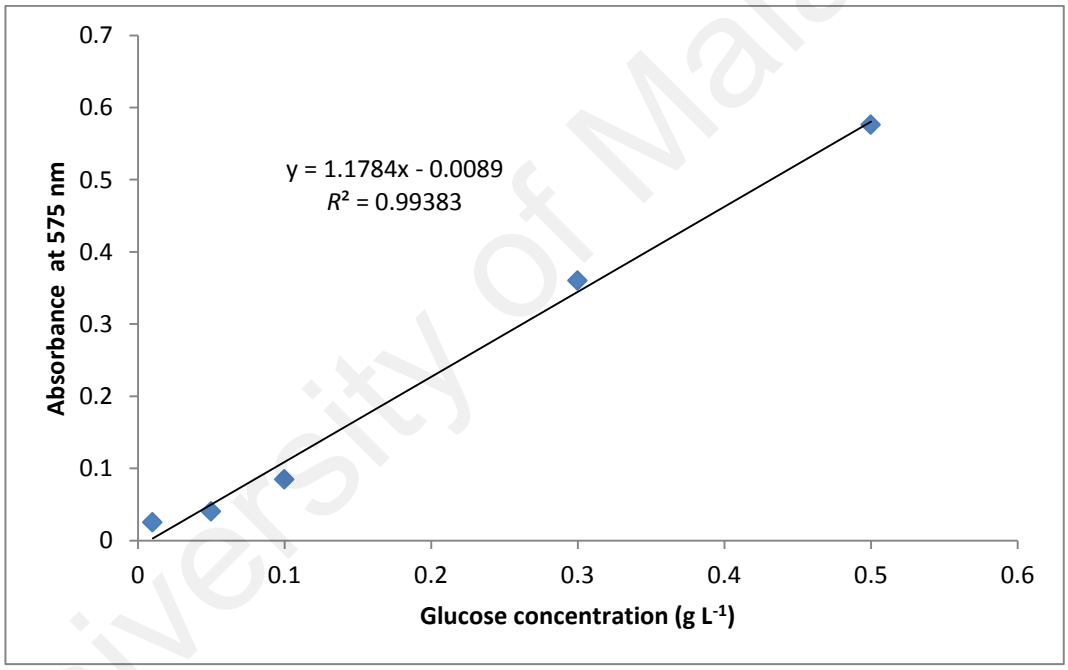

Figure 4.2 Glucose standard calibration

4.3 SCREENING OF SELECTED SONICATION PARAMETERS

The effects of selected sonication parameters i.e sonication intensity (W cm^{-2}), irradiation time (min), xanthan gum concentration (g L^{-1}) and NaCl solution concentration (M) on xanthan gum degradation were screened using full factorial design (FFD). A total of 48 experimental combinations of full factorial design at the lowest and highest levels sonication factors were shown in Table 4.2 below.

Table 4.2 Experimental combinations for FFD

Run Order	Sonication Intensity (W cm^{-2})	Irradiation time (minutes)	Concentration of xanthan gum (g L^{-1})	Concentration of NaCl (M)	Degree of degradation (%)
1	11.5	30	1	0.1	0.89
2	11.5	120	5	0	3.78
3	11.5	120	1	0	11.18
4	2.7	30	5	0	0.90
5	2.7	30	5	0.1	0.65
6	11.5	120	5	0.1	3.06
7	2.7	120	1	0.1	1.43
8	11.5	120	5	0	3.83
9	11.5	120	1	0	10.91
10	11.5	120	1	0.1	6.62
11	2.7	120	1	0	5.81
12	2.7	30	5	0.1	0.61
13	2.7	30	1	0	0.45
14	11.5	120	5	0.1	3.11
15	2.7	120	1	0.1	1.61
16	2.7	30	1	0.1	0.09
17	11.5	120	5	0.1	3.11
18	11.5	30	1	0.1	0.80
19	11.5	120	1	0	10.73
20	11.5	30	5	0.1	0.00
21	11.5	30	5	0.1	0.00
22	2.7	120	5	0	1.52

23	2.7	30	1	0	0.54
24	11.5	120	1	0.1	6.35
25	11.5	30	1	0	0.45
26	2.7	120	1	0	5.63
27	2.7	30	5	0	0.90
28	2.7	120	5	0	1.41
29	2.7	120	5	0.1	1.66
30	2.7	120	5	0.1	1.65
31	11.5	30	5	0.1	0.00
32	2.7	30	5	0.1	0.86
33	2.7	30	1	0.1	0.09
34	2.7	120	1	0	5.46
35	2.7	30	1	0	0.54
36	11.5	30	1	0	0.45
37	11.5	30	5	0	1.16
38	11.5	120	5	0	3.79
39	2.7	120	5	0	1.32
40	11.5	30	1	0	0.54
41	2.7	120	1	0.1	1.25
42	11.5	30	5	0	1.20
43	2.7	120	5	0.1	1.83
44	11.5	120	1	0.1	6.53
45	11.5	30	1	0.1	0.98
46	2.7	30	5	0	0.95
47	11.5	30	5	0	1.16
48	2.7	30	1	0.1	0.09

The response used i.e. degree of degradation produced by a change in the level of these factors was modelled using full-order polynomials shown below (Equation 4.1) where A_0 and A_i/A_{ij} represented general mean and regression coefficient corresponding to the main factor effects/interactions, respectively.

$$\begin{aligned}\textit{Degree of degradation (\%)} = {} & A_0 + A_1X_1 + A_2X_2 + A_3X_3 + A_4X_4 + A_5X_1X_2 \\ & + A_6X_1X_3 + A_7X_1X_4 + A_8X_2X_3 + A_9X_2X_4 \\ & + A_{10}X_3X_4 + A_{11}X_1X_2X_3 + A_{12}X_1X_2X_4 \\ & + A_{13}X_1X_3X_4 + A_{14}X_2X_3X_4 + A_{15}X_1X_2X_3X_4 \end{aligned} \quad (4.1)$$

4.3.1 Analysis of FFD experiments on screening of sonication parameters

Analysis of variance (ANOVA) (Table 4.3) of full order model terms showed the effects of the main factors and their interactions were all significant (p<0.05). This was supported by the normal plot of the standardized effects that showed all factors (main and interactions) were significant towards the response (Figure 4.3). Irradiation time showed the most pronounced effects on the response (F = 14193.14), followed by sonication intensity (F = 3353.56), concentration of xanthan gum (F = 2980.01) and concentration of NaCl (F = 1745.37). Both correlation coefficient, R^2 and adjusted R^2 were determined at 99.91 % and 99.86 % respectively.

Table 4.3 ANOVA analysis for the effects of sonication parameters

Factor	Degree of freedom	Adjusted sum of squares	Adjusted mean of square	*F*	*P*
Main factor	4	255.1	63.8	5568.02	0.000
Intensity		38.4	38.4	3353.56	0.000
Time		162.6	162.6	14193.14	0.000
Conc. xanthan gum		34.1	34.1	2980.01	0.000
Conc. NaCl		20.0	20.0	1745.37	0.000
2-way interactions	6	108.9	18.2	1584.77	0.000
*Intensity * Time*		34.9	34.9	3051.19	0.000
*Intensity * Conc. xanthan gum*		11.2	11.2	981.55	0.000
*Intensity * Conc. NaCl*		0.3	0.3	29.84	0.000
*Time * Conc. xanthan gum*		43.0	43.0	3751.6	0.000
*Time * Conc. NaCl*		10.8	10.8	942.89	0.000
Conc. xanthan gum Conc. NaCl*		8.6	8.6	751.52	0.000
3-way interactions	4	23.7	5.9	517.93	0.000
*Intensity * Time * Conc. xanthan gum*		5.3	5.3	466.34	0.000
*Intensity * Time * Conc. NaCl*		0.2	0.2	19.47	0.000
*Intensity * Conc. xanthan gum* Conc. NaCl*		1.2	1.2	104.8	0.000
*Time * Conc. xanthan gum* Conc. NaCl*		17.0	17.0	1481.09	0.000
4-way interactions	1	0.2	0.2	17.42	0.000
*Intensity * Time * Conc. xanthan gum* Conc. NaCl*		0.2	0.2	17.42	0.000
Error	32	0.367	0.011		
Total	47	388.289			

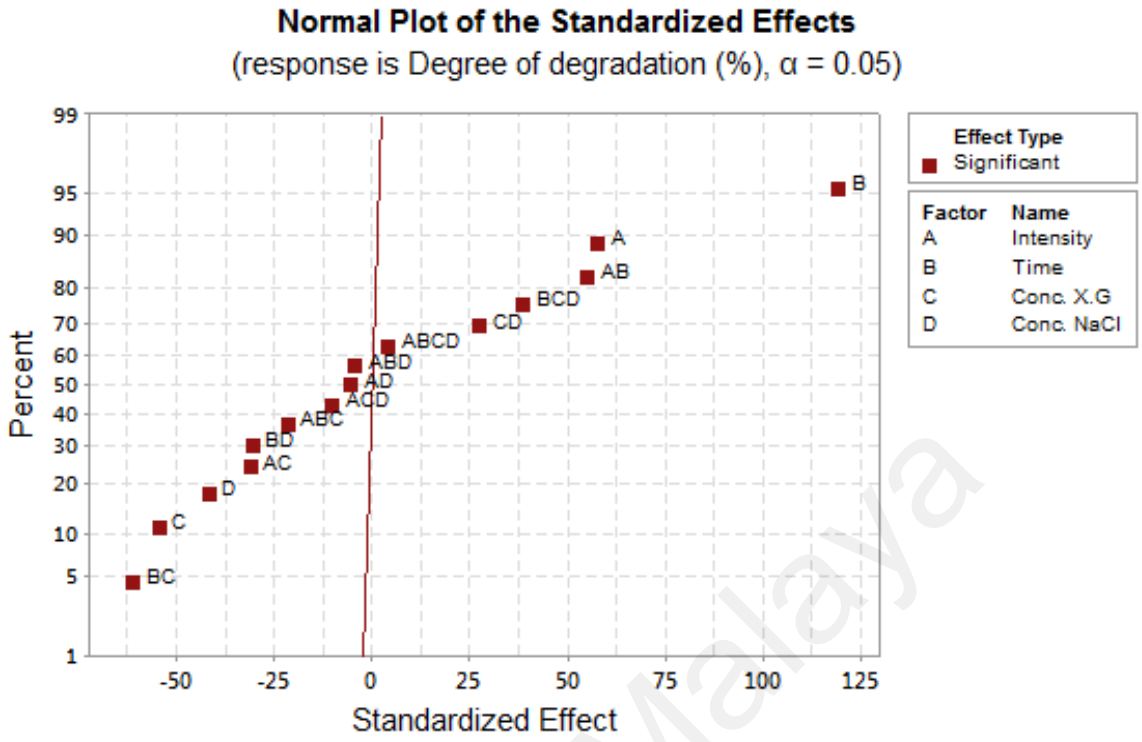

Figure 4.3 Normal plot of the standardized effects of sonication parameters

4.3.2 Residual analysis

The normality of the experimental data was assessed using residual plots as shown in Figure 4.4. From the normal probability plot (Figure 4.4*a*), all standardized residuals were distributed well along the theoretical normal distribution line and in agreement with the general bell-shaped curve of the histogram (Figure 4.4*b*), thus diminishing the probability of non-random error contributing to the observed effects. No potential outliers were detected as all the points generally fell randomly and equally on both sides of standardized zero line within the range ± 3.0 (Figure 4.4*c*). In addition, the absence of systematic error in the experiment was also indicated by random pattern of data scattering in the plot (Figure 4.4*c*). Furthermore, random pattern in the standardized residuals versus observation order plot (Figure 4.4*d*) indicated that the sequence of the experiments did not contribute to detectable systematic error i.e. the data obtained was expected to be independent of the order of its collection. Thus, it can

be concluded that the experimental data fitted to the full term model followed normal distribution pattern, and they were less likely to be influenced by non-random or systematic error.

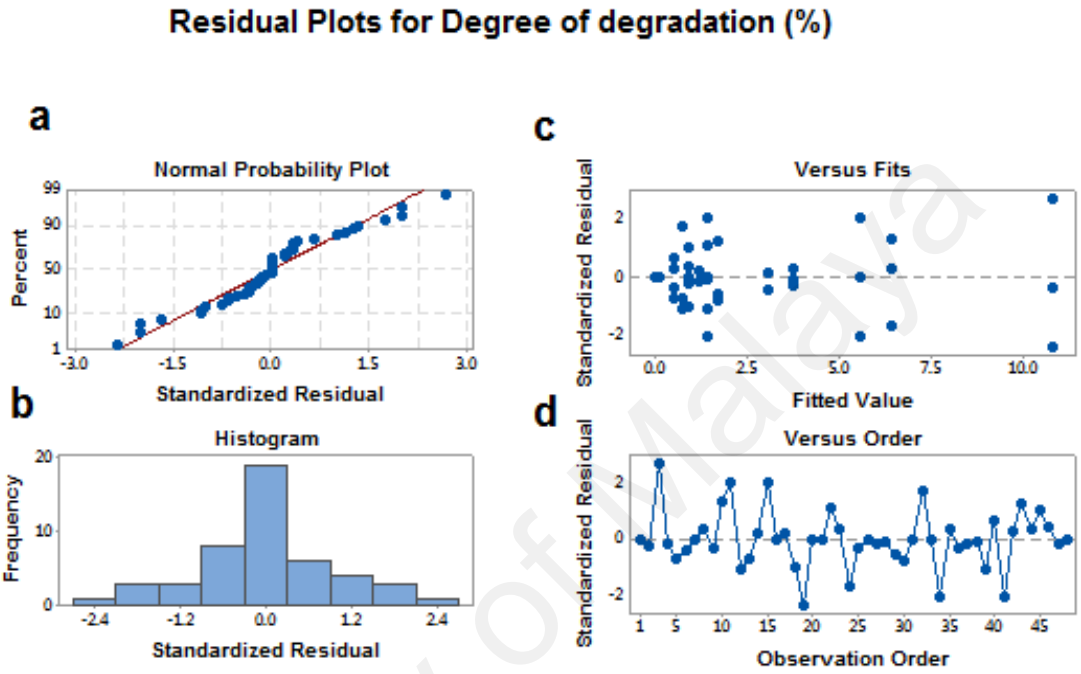

Figure 4.4 Residual plots for the data on the effects of sonication parameters

4.3.3 Main effect plots

The main effects of selected sonication parameters on the degree of xanthan gum degradation were shown in the corresponding plot (Figure 4.5). Sonication intensity and irradiation time showed positive significant effects as can be seen from the increment of the degree of degradation (%) when each factor was changed from low to high levels (Figure 4.5*a*&*b*). In contrast, at high levels of xanthan gum concentration (g L^{-1}) (Figure 4.5*c*) and salt concentration (M) (Figure 4.5*d*), a reduction in degradation efficiency was observed indicating their negative effects on the response. Hence, it is hypothesized that efficient degradation could be achieved at high sonication intensity (11.5 W cm^{-2}),

irradiation time 120 min, low initial concentration of xanthan gum (1.0 g L^{-1}), and excluding or reducing NaCl concentration (< 0.1 M) in the solution.

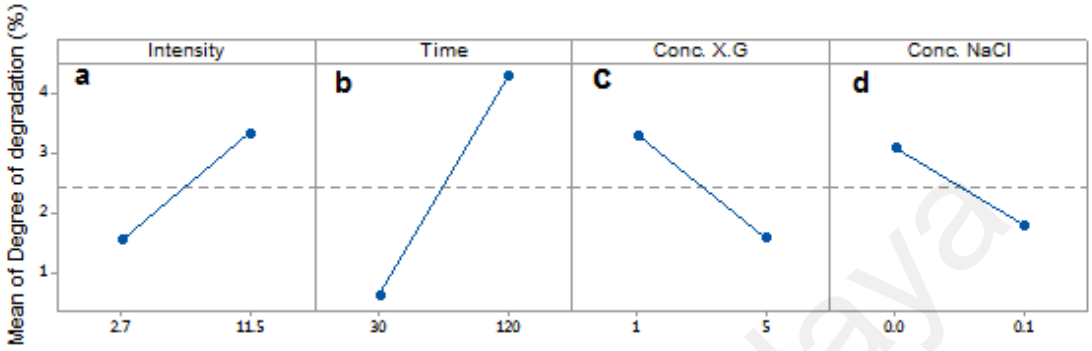

Figure 4.5 Main effects plot

4.4. OPTIMIZATION

To obtain optimum concentrations of xanthan gum and NaCl solutions, reduced concentration ranges were investigated i.e. (g L^{-1}) 0.1, 0.5, 1.0 and 5.0 for xanthan gum solution and (M) 0, 1.0×10^{-4}, 1.0×10^{-3}, 1.0×10^{-2}, 1.0×10^{-1} for NaCl solution, following the direction of degree of degradation as shown in the main effects plot (Figure 4.5*c*&*d*). Sonication time and intensity were fixed at 120 min and 11.5 W cm^{-2} respectively. The factors were investigated sequentially, starting with xanthan gum, followed by NaCl. A published study claimed that different salt concentrations in xanthan gum solution affected the degradation rate differently (Li & Feke, 2015). A reduction in degradation rate was observed as the molar concentration of NaCl solution increased. However, the fastest degradation rate was achieved in 10^{-4} M NaCl solution, almost 30 % faster than salt-free solutions. Hence, this investigation sought to confirm the reported effect of NaCl concentration on xanthan gum degradation

4.4.1 Effect of xanthan gum concentration

It was shown that the increase in xanthan gum concentration resulted in significantly reduced degree of degradation (Table 4.4). When the gum concentration was increased five-fold, the degree of degradation reduced drastically from 39.8 % to 5.8 %, and was further reduced when the concentration > 0.5 g L^{-1}. It was also observed that the increase in concentration was accompanied by significant increase in the solution viscosity, where the lowest concentration of 0.1 g L^{-1} showed low viscosity at 1.1 mPa.s, and relatively high viscosity at 93 mPa.s when the xanthan gum concentration was increased fifty-folds. To initiate cavitation in a liquid, the negative pressure imposed by the acoustic wave during the rarefaction cycle must be large enough to overcome the natural cohesive forces holding the liquid together, a limit known as cavitation threshold. However, as the viscosity of the liquid increases, the natural cohesive force of the liquid becomes stronger hence increasing the cavitation threshold of the liquid simultaneously (Lorimer & Mason, 2002). As a result, cavitation is harder to achieve in viscous xanthan gum solution leading to smaller degree of degradation of the polymer chain. Similar results have been achieved by Kasaai *et al.* (2008) on chitosan i.e. at constant power output of 71.3 W, 25 °C for 15 min, the chain scission obtained was inversely proportional to chitosan concentration ranging from 0.2 to 1.0 % (w/v). Since higher concentration of solution results in higher viscosity, some amount of energy released from the collapse of the microbubbles is used to dis-aggregate the molecules, and the subsequent propagation of ultrasonic wave is less impactful in dilute regime of the solution leading to smaller magnitude of degradation. Mohod and Gogate (2011) investigated the effect of concentration on ultrasound-mediated degradation of CMC solution. Different concentrations of 0.1, 0.2, 0.3 and 0.5 % (w/v) carboxymethylcellulose (CMC) were sonicated at constant liquid volume and ultrasonic power. It was reported that the maximum degradation rate constant was

achieved at the lowest concentration of CMC solution. This was attributed to the less mobile molecules in viscous polymer system when CMC concentration was high, hence resulting in a smaller velocity gradient in the vicinity of the collapsing bubbles thus minimizing the probability of polymer chain breaking. Harkal *et al.* (2006) also indicated that 1.5 % (w/w) concentration was the optimum concentration of poly(vinyl alcohol) in aqueous solution, beyond which the extent of degradation was reduced. Similarly, this was attributed to the depressed cavitation intensity due to the changes in the solution physical properties with respect to the increasing polymer concentration.

Table 4.4 Degree of degradation as a function of xanthan gum concentration and its viscosity

Concentration of xanthan gum (g L^{-1})	**Viscosity (mPa.s)**	**Degree of degradation (%)**
5	92.5 ± 0.14	1.4
1	7.1 ± 0.12	2.8
0.5	2.6 ± 0.03	5.8
0.1	1.1 ± 0.01	39.8

4.4.2 Effect of NaCl concentration

From the results, the highest degradation of xanthan polymer was achieved in the absence of NaCl in the solution, while the least was obtained in the highest concentration of NaCl i.e. 0.1 M (Table 4.5). Consequently, the highest degradation was observed in very low ionic strength solution (salt-free), and as the ionic strength of the solution increases as a function NaCl molar concentration, the degree of degradation started to decline to approximately 4 % at 0.1 M NaCl, I = 0.1 M (Table 4.5). It is also interesting to note that at a very low NaCl concentration used i.e. 1.0×10^{-4} M ($I = 1.0 \times 10^{-4}$ M), a significant reduction in degree of degradation was observed relative to salt-free solution. Furthermore, when the NaCl molar concentration was increased by an order of magnitude ($M = 1.0 \times 10^{-3}$, $I = 1.0 \times 10^{-3}$ M), no significant different in the

degree of degradation was observed. This indicated that the presence of high amount of dissociable salt such as NaCl lowered the degree of degradation of xanthan polymer, and there exists a range of molar concentration (and ionic strength) of the salt where its effect on the degree of degradation is similar, as shown by the results.

The anticipated effect of ionic strength of salt in the solution of xanthan gum is attributed to the changes in conformational structure of xanthan polymer. Low charge-density ions such as NaCl was selected in this study based on its salting out ability that supposedly aids in the degradation process based on the findings reported by Li and Feke (2015). The finding in this study however, was in contradiction to the earlier published report. Recent finding by Schaefer *et al.* (2016) has proven that the contour length, rather than the mass of polymer is the main parameter in the stretch-and-break mechanism for ultrasound-mediated degradation of polymer. Polymers of the same length but with different effective mass exhibit identical scission characteristics upon ultrasonication in solution. This breakthrough finding could explain the phenomena of the sonication ineffectiveness in high salt concentration solution of xanthan gum. We hypothesized that the low degree of xanthan gum degradation recorded in the highest concentration of NaCl solution was directly attributed to its contour length that decreases upon increasing salt concentration. Camesano and Wilkinson (2001) determined that in salt-free solution, the number average contour length, L_c of xanthan polymer is 1651 nm and decreases to 575 nm when exposed to 0.1 M KCl and further decreasing to 450 nm in 0.5 M KCl. This reduction in contour length upon exposure to high ionic concentration is associated with the formation of flexible chain as observed under atomic force microscopy (AFM) carried out by the researchers. This change in conformational structure upon addition of salt is attributed to the intramolecular interaction. Since both xanthan backbone and its side chain are negatively charged, the intramolecular electrostatic repulsion is high when dissolved in ionic–free solution

hence forcing this molecule to stretch in order to minimise this repulsive interactions, increasing its chain stiffness. Increasing the ionic strength in the aqueous solution causes reduction in intramolecular charge repulsion and causes the rigid conformation to collapse (Roller & Jones, 1996). Using renatured xanthan, the researchers obtained a measured persistence length, L_p of 417 nm in salt-free solution, and this was reduced to 168 nm in 0.5 M KCl. Thus, in the presence of salt, the rigidity of the polymer decreases, xanthan become more flexible and bending of the contour length started to occur giving a lower value of persistence length. Similar trend of contour length, L_c changes was observed on native commercial xanthan, which was also used in this study, by Chun and Park (1994). They investigated the molecular shape of xanthan in NaCl solution ranging from 2.0×10^{-4} to 1.0×10^{-1} M concentration. In the lowest ionic concentration solution, the contour length, L_c measured was 0.88 µm and it decreases to 0.58 µm in the highest ionic concentration solution. Therefore the lower degree of xanthan degradation obtained at high concentration of NaCl in this study could be attributed to the shortening of contour/persistence length of the polymer that limit the effectiveness of chain scission. The coiling effect, induced by the presence of salt ions and contributed by increased flexibility of the xanthan polymer, thus helped to shield backbone of the chain from the shear force generated by collapsing microbubbles.

Table 4.5 Degree of degradation as a function of different molar concentrations of NaCl in 0.1 g L^{-1} xanthan solution

Concentration of NaCl (M)	Ionic strength, *I* (M)	Degree of degradation (%)
No salt	~ 0	32.7
1.0×10^{-4}	1.0×10^{-4}	25.6
1.0×10^{-3}	1.0×10^{-3}	25.5
1.0×10^{-2}	1.0×10^{-2}	12
1.0×10^{-1}	1.0×10^{-1}	4.4

4.5 ANALYSIS ON DEGRADED XANTHAN GUM

4.5.1 Molecular weight analysis

Molecular weight analysis was performed on ultrasound-irradiated xanthan gum using SEC to further investigate the extent of degradation on this physical property of xanthan gum. The SEC chromatogram profiles of sonicated xanthan gum were shown in Figure 4.6. No formation of secondary peak was observed. The peak started to broaden gradually over time and this effect was evident immediately after 1 min of irradiation. Low molecular weight fractions were eluted out later hence the peak broadening shown in the chromatogram. The low molecular weight fractions accumulated over time. However, towards the later stage of sonication, the peak width started to narrow down as very little remaining large fragments were eluted out beyond 8 minutes of retention time due to the generation of the low molecular weight fractions. This indicated that xanthan polymer population has undergone scission to yield fragments with similar sizes at which no further scission action took place. The average size of the fragments population, designated as limiting molecular weight, was at 358×10^6 g mol^{-1}.

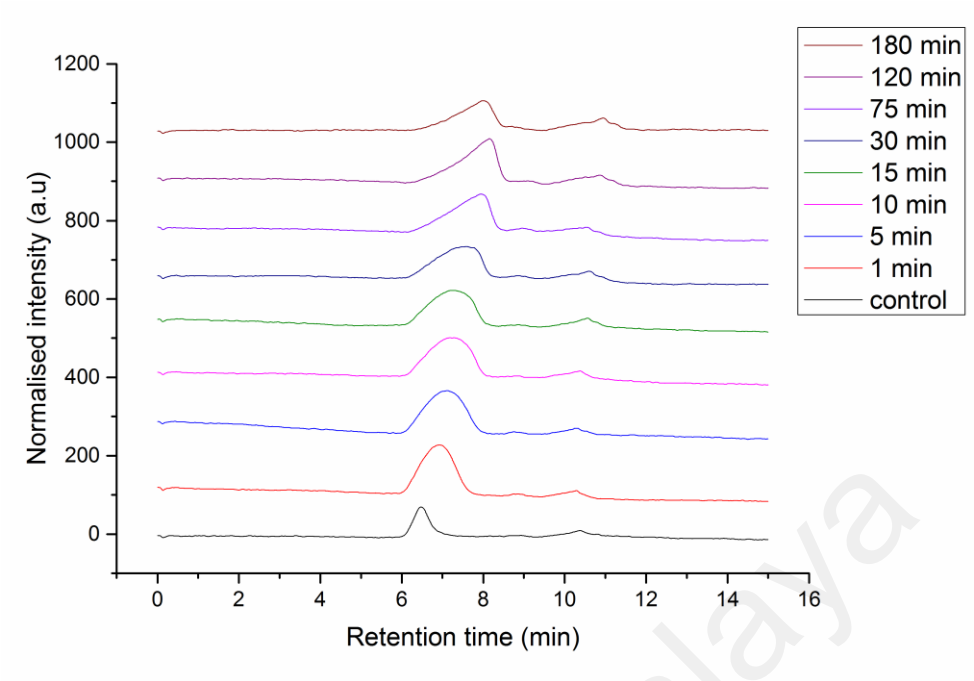

Figure 4.6 SEC chromatogram of 0.1 g L^{-1} xanthan gum solution sonicated at 11.5 W cm^{-2} excluding the NaCl

The limiting molecular weight, where the corresponding fragments no longer undergo scission under ultrasonic conditions that would normally caused chain breakage, was further evidenced by studying the profile of molecular weight change against irradiation time for xanthan gum solution (Figure 4.7). It was indicated by the plateau section of the profile for 0.1 g L^{-1} xanthan in salt-free solution irradiated at 11.5 Wcm^{-2} intensity. The reduction of xanthan polymer number average molecular weight (M_n) was best described by second order exponential decay as shown below (Equation 4.2):

$$y = y_0 + A_1 exp^{-x/t_1} + A_2 exp^{-x/t_2} \quad (4.2)$$

where y_0 represents the limiting molecular weight, and $^1/t_1$, and $^1/t_2$ represent rate constants for different segments of the decay profile. Post-fitting analysis showed the correlation coefficient, R^2 = 0.996, adjusted R^2 = 0.9963 and root-mean-square deviation (RMSD) = 56.95 which supported satisfactory modelling of molecular weight data.

Two different rate constants can be calculated for the different segments of the profile according to Equation (4.2). A significant and very fast molecular weight reduction at the rate of 14.6×10^{-2} s^{-1} was observed at the initial segment of the profile, and this rapid reduction corresponded to a weight loss of almost 50 % within five seconds of irradiation. The initial xanthan polymer chain scission rate was the fastest, and as the mechano-chemical effects by sound wave became gradually less pronounced with sonication time (Czechowska-Biskup *et al.*, 2005), slower rate of 6.1×10^{-4} s^{-1} towards the end of sonication process was observed. It can be concluded that larger molecules at the start of irradiation were more susceptible to the extreme sonication-induced hydrodynamic forces. Thus, a typical molecular weight profile of ultrasound-irradiated xanthan polymer will eventually levelled off to a constant value, designated as limiting molecular weight, below which polymer fragments seems to be unaffected by the ultrasound irradiation.

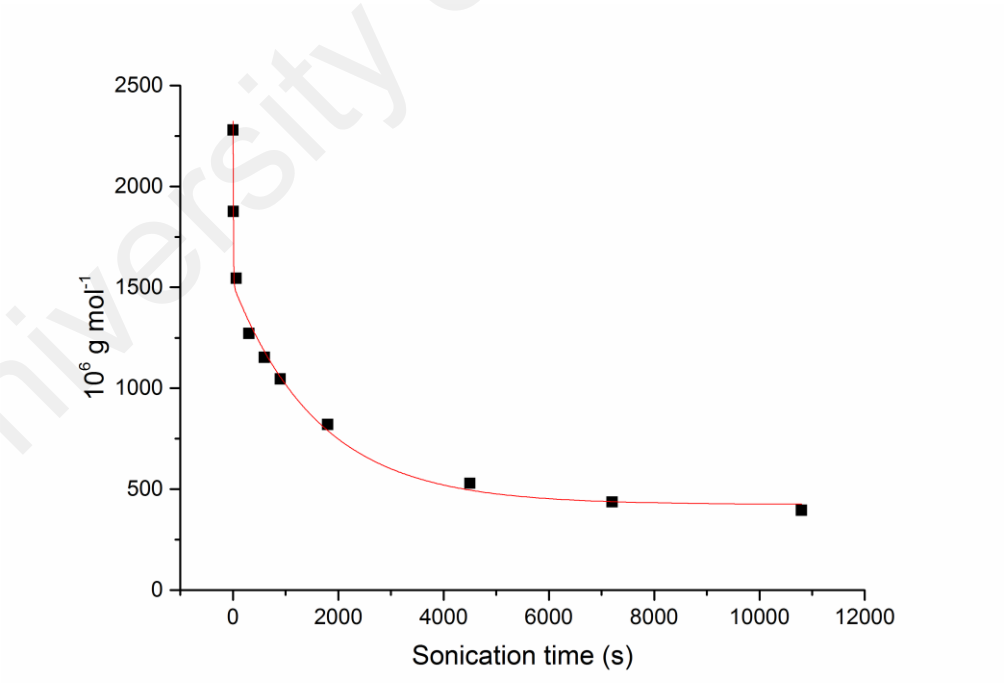

Figure 4.7 Decreasing number average molecular weight (M_n) as a function of irradiation time

An investigation on the limiting molecular weight was extended to ultrasonication of xanthan solutions at 0.1 and 1 g L^{-1} in salt-free solutions, and at 0.1 g L^{-1} in 0.1 M NaCl solution. The results obtained were shown in Figure 4.8. Optimum sonication intensity at 11.5 W cm^{-2} and irradiation time 180 minutes were applied. From the results, xanthan at 0.1 g L^{-1} in salt-free solution showed the lowest limiting molecular weight i.e. 358 × 10^6 g mol^{-1} among the three conditions tested. At 1.0 g L^{-1} xanthan in salt-free solution, the limiting molecular weight was determined at 436 × 10^6 g mol^{-1}. This value was not significantly different from the limiting molecular weight determined at 0.1 g L^{-1} xanthan i.e. 480 × 10^6 g mol^{-1}, but in the presence of 0.1 M NaCl. This observation lends further support to the effect of dissociable salts as discussed earlier. In addition, the results suggested that the limiting molecular could be adjusted to some extent by incorporating salts such as NaCl.

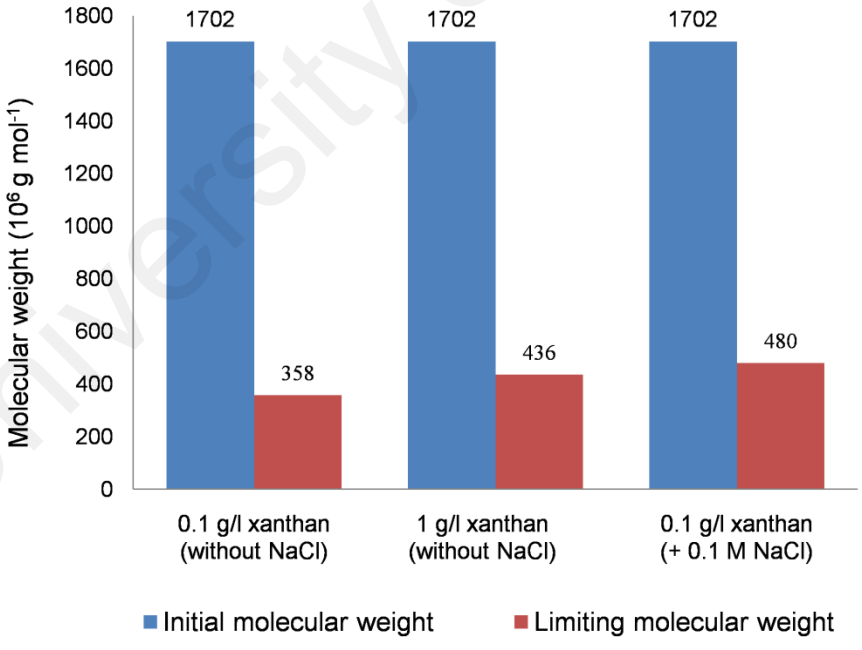

Figure 4.8 Limiting molecular weight as a function of xanthan concentration and the presence of NaCl

4.5.2 Modeling of xanthan polymer degradation under ultrasound irradiation

In order to verify the scission mechanism of ultrasonic degradation on xanthan gum, two different scission models were fitted to the data profile of xanthan polymer chain scission namely random and midpoint scission models. Random scission polymer degradation model was developed by Schmid (1940) (Equation 4.3) assuming the scission occurs randomly and the rate of degradation decreases with decreasing chain length, giving:

$$\frac{M_e}{M_t} + \ln\left(1 - \frac{M_e}{M_t}\right) = -\frac{k_1}{c}\left(\frac{M_e}{m}\right)^2 xt - \frac{M_e}{M_i} + \ln(1 - \frac{M_e}{M_i}) \qquad (4.3)$$

while midpoint chain scission is assumed to occur at the midpoint of the polymer chain (Equation 4.4) (Madras *et al.*, 2000);

$$\ln\left[\frac{M_i - M_e}{M_t - M_e}\right] = k_2 M_e t \qquad (4.4)$$

where M_i, M_e, and M_t are initial M_n, final M_n and M_n at time t, m is the molecular weight of the monomer, c is the initial molar concentration, and k_1 or k_2 is the degradation rate constant, respectively.

It was found that midpoint scission model fitted the experimental data better compared to the random model (Figure 4.9). Post-fitting analyses for both models were shown in Table 4.6. Hence, it is hypothesized that under ultrasonic irradiation, xanthan polymer degradation in aqueous solution followed midpoint scission model where chain breaking occurred at the midpoint of the polymer length, and continued until the limiting molecular weight is reached.

Table 4.6 Post-fitting analysis for midpoint- and random chain scission models

Scission model	R^2	Adjusted R^2	RMSD	Variance (σ)
Midpoint chain scission	0.9997	0.9996	0.0076	0.0005
Random chain scission	0.9577	0.9471	0.0425	0.0162

RMSD: root-mean-square deviation

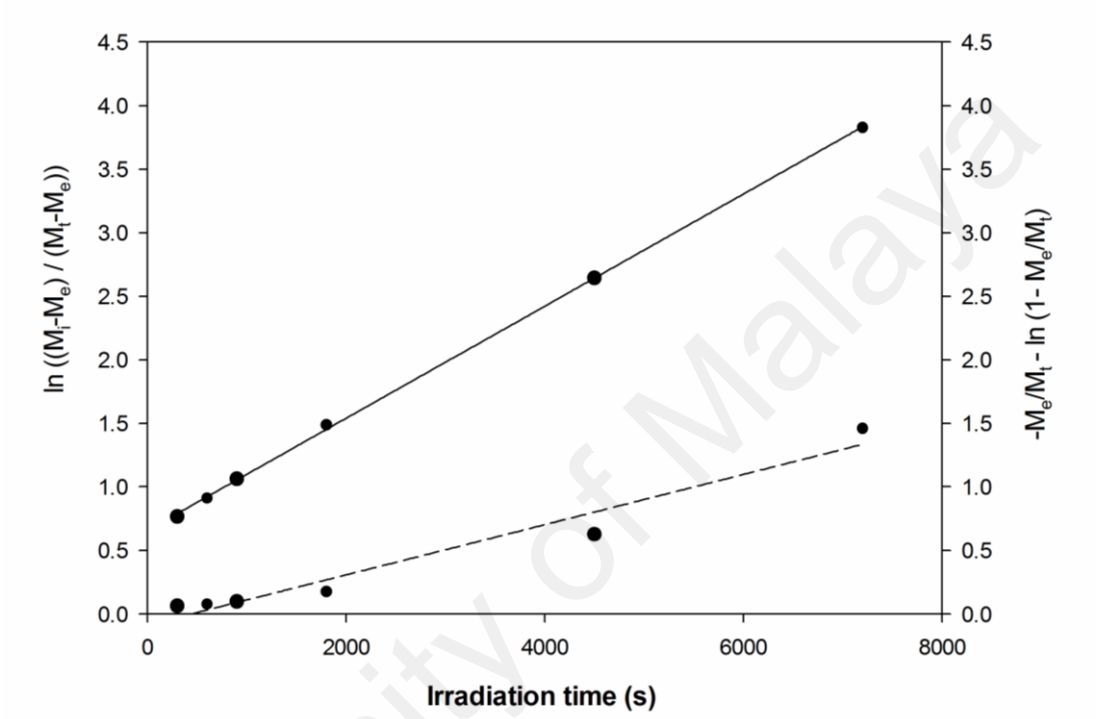

Figure 4.9 Fitting of experimental data by random (dashed line) and midpoint (solid line) chain scission model

4.5.3 Thermogravimetric analysis (TGA)

The thermal decomposition of non-sonicated and sonicated xanthan gum at increasing irradiation time was analysed to support the midpoint scission theory pointed previously. Derivative TGA (*d*TGA) curves of xanthan polymer were shown in Figure 4.10. The first mass loss peak was associated with water content loss in xanthan, absorbed through its polar functional groups (Faria *et al.*, 2011). The decreasing decomposition temperature recorded together with the reduction in derivative weight as sonication time increases showed that the initial bulk polymer was fragmented over time. The smallest fragments produced after 120 min of sonication needed the least heat transfer to start decomposing as shown from the broadening of the peak (Figure 4.10). Scission at the midpoint of xanthan gum will create fragments of approximately similar sizes; hence only single major decomposition peak would be obtained as shown in Figure 4.10, after neglecting the mass loss peak due to dehydration. Thus, the *d*TGA data lends support to the conclusion that xanthan polymer breaks at the mid-section of its length following exposure to acoustic force.

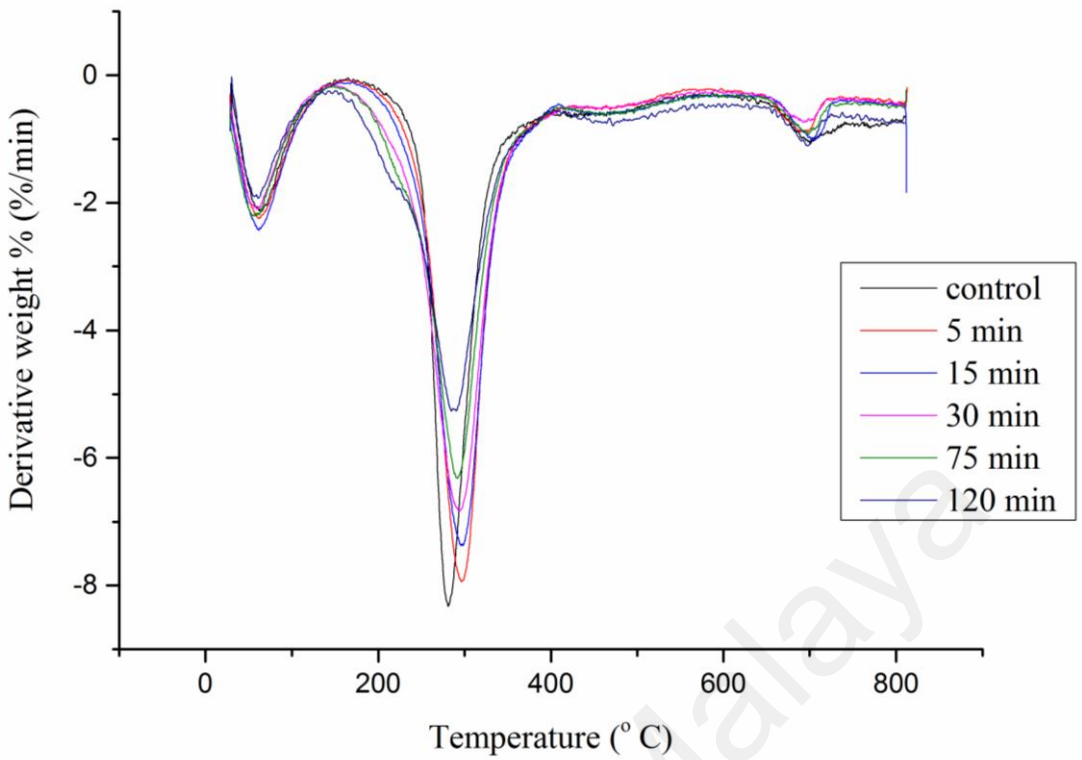

Figure 4.10 Derivative TGA curve of control and sonicated salt-free xanthan aqueous solution at 0.1 g L^{-1}, 11.5 W cm^{-2}, 120 min

4.5.4 Fourier Transform Infrared Spectroscopy (FTIR)

To investigate the ultrasonic scission site of action on xanthan gum, FTIR was performed to determine any alteration in xanthan gum structure if present. FTIR spectra of control and sonicated xanthan gum samples are shown in Figure 4.11 with its corresponding peaks wave number described in Table 4.7. The broad band region from 3567 – 3057 cm^{-1} was attributed to stretching vibration of O-H carbohydrate group and hydrogen bonds (Poletto *et al.*, 2014). The decrease in intensity signal of this band region after 120 min of sonication was attributed to the loss of hydrogen bonding when exposed to the high intensity acoustic wave (Yuen *et al.*, 2009). In xanthan polymer, intra-molecular hydrogen bonding occurs between methyl residues of acetate group at the side chain with adjacent oxygen atom of D-glucose at the main chain. Hydrogen bonding between the alternate hydroxyl group at C-3 and the adjacent oxygen atom of

the D-glucosyl residue contributes to the rigid structure of xanthan cellulose backbone (Tako & Nakamura, 1989; Tako *et al.*, 2014). The –C=O stretching of pyruvate, acetate and glucoronate signal was assigned to band region between 1725 - 1615 cm^{-1} (Faria *et al.*, 2011). Reduced peak intensity and slight shifting of this peak was observed in sonicated xanthan gum samples (Figure 4.11) correlated well with the functional groups located at the side chain affected by high shear force of collapsing bubbles following compression cycle of the sonication.

Structural information was obtained from two different band regions namely sugar region (1200 - 950 cm^{-1}) and anomeric region (950 - 750 cm^{-1}). The former region is represented by highly overlapping intense bands of C-O and C-C stretching vibrations in glycosidic bonds and pyronoid ring while anomeric region was described by the weak bands of complex skeletal vibrations sensitive to anomeric structure (Synytsya & Novak, 2014). The bands in regions 845 - 810 and 900 - 890 cm^{-1} were assigned to vibrations of equatorial (α anomer) and axial (β anomer) C-1-H group respectively (Tul'chinsky *et al.*, 1976). No vicissitudes in signal intensity of sugar region were observed following sonication, which indicated the presence of glycosidic bond. However, a reduction in intensity signal was observed at α anomeric C-1-H group band located at around 804 cm^{-1}. α anomeric C-1-H group was found in mannose, a component of xanthan side chain located next to the main chain. Since spectrum in the anomeric region is suitable for the determination of the configuration of the glycosidic bond (Tul'chinsky *et al.*, 1976), it was suggested that scission might also have occurred at 3-1 linked α glycosidic bond that connects the main chain to the side chain.

The 700 - 500 cm^{-1} region can be defined as the region of crystallinity. There are bands caused by non-planar, bending modes of hydroxyl groups participating in hydrogen bond formation (Tul'chinsky *et al.*, 1976). Continued losses of hydrogen bonds in sonicated samples will lead to a lowering of crystallinity, as can be seen from

the reduced signal intensity in this region. This region however may also be attributed to other vibrations, especially those involved in skeletal vibrations (Synytsya & Novak, 2014; Yuen *et al.*, 2009).

Table 4.7 FTIR spectral data of control and sonicated xanthan gum samples in salt-free solutions at 11.5 W cm^{-2} power intensity (cm^{-1})

	Control	**Sonicated xanthan**
1. -OH stretching	3567-3057	3558-3048
2. -CH stretching, CH2 and CH3- symmetric and asymmetric	2974-2880	2974-2880
3. -C=O stretching (pyruvate, glucoronate and acetate)	1725-1615	1712-1616
4. C-H bending (CH_2 and CH_3 deformation) & O-C-H, C-C-H, C-O-H bending	1465-1267	1465-1267
5. C-O and C-C stretching (sugar region)	1110 -1023	1110 -1023
6. Anomeric region	901-734	901-734
7. Crystallinity region	734-550	734-550

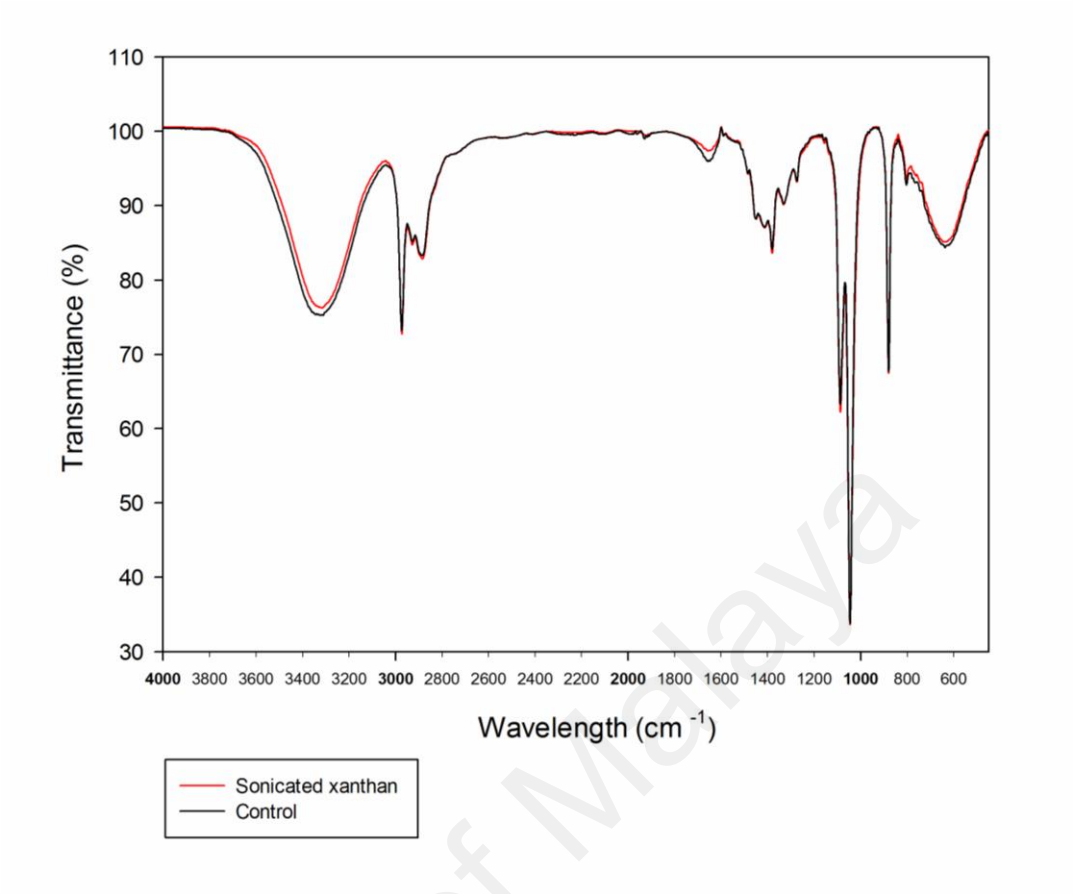

Figure 4.11 FTIR spectra of control and sonicated xanthan gum samples in salt-free solutions

4.5.5 Differential Scanning Calorimetry (DSC)

Differential scanning calorimetry (DSC) was performed to investigate the thermal properties of ultrasound irradiated xanthan gum samples in salt-free and 0.1 M NaCl solutions. DSC thermogram of control and sonicated xanthan gum samples are shown in Figure 4.12. It was clear that there was a reduction in melting temperature (T_m) of xanthan sample when exposed to 11.5 W cm^{-2} power intensity for 30 min in salt-free solution. The enormous shear force generated from the collapsing bubbles creates the micro-streaming effects on polymer in close proximity hence generating fragments of the native polymer chain. The intermolecular entanglement within the polymer mixture was also likely to be reduced hence its reduced T_m. However, similar reduction trend in T_m was not observed for xanthan gum samples in 0.1 M NaCl solution when exposed to ultrasound irradiation under similar conditions. When the ionic strength was

increased, electrostatic repulsion between charged groups was screened (Fitzpatrick *et al.*, 2013) leading to the T_m peak being shifted to a higher temperature due to the stabilised helical structure from the folding of side chain around the xanthan polymer backbone. The polymer was therefore less susceptible to the degrading effects of ultrasound irradiation as opposed to xanthan gum samples in salt-free solutions.

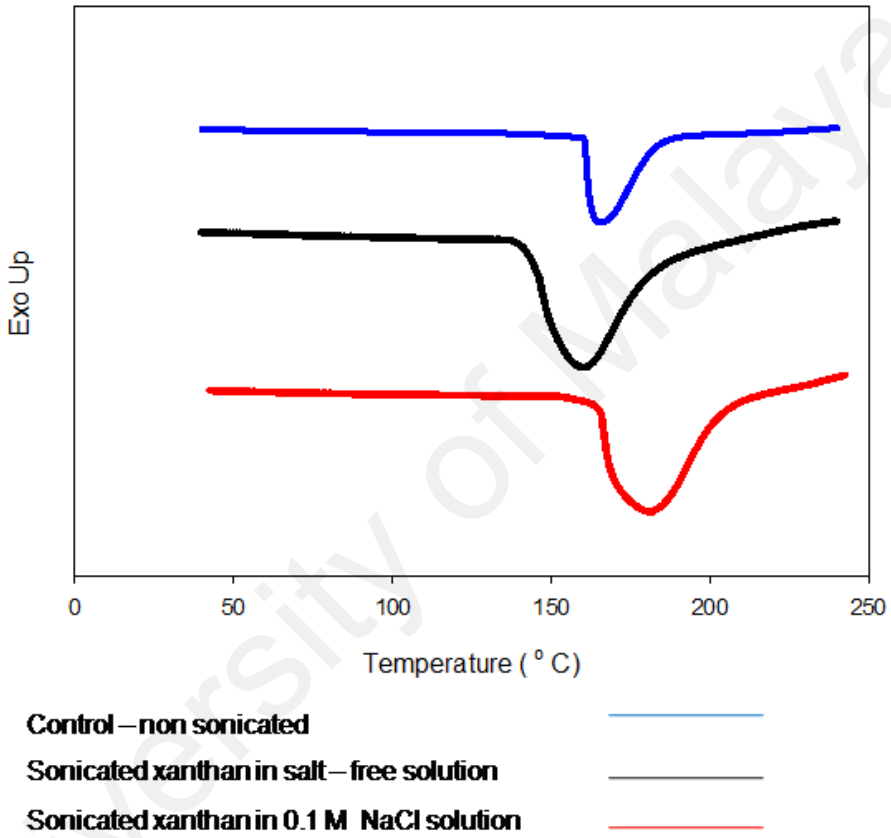

Figure 4.12 DSC thermograms of control and sonicated xanthan gum samples exposed to 11.5 W cm^{-2} power intensity for 30 min

4.5.6 ^{1}H-NMR Spectroscopy

The condition of xanthan gum side chains after degradation was studied using ^{1}H-NMR. Proton NMR spectra of xanthan gum samples are shown in Figure 4.13. Peak *a* corresponded to the equatorial alpha anomeric proton of mannopyranosic unit carbon, known to be the more de-shielded proton located at 5.2 ppm. Peaks *b* and *c* were

assigned to proton signal of acetate and pyruvate respectively. The quantification of pyruvate and acetate on xanthan side chain was made *via* integration of these substituents proton signal with reference to the anomeric proton, peak *a* (Rinaudo *et al.*, 1983). The proton signals from unsonicated xanthan gum samples however, were not detectable. The rigid molecular conformation of the native xanthan gum resulted in strong dipole interactions between the nucleus of hydrogen and the nucleus of carbon leading to the enlargement of the resonance line (Faria *et al.*, 2011). From Figure 4.13, it was found that the intensity ratio of signal *a* (proton of equatorial alpha anomeric carbon) to signal *b* (proton of acetate) was reduced when xanthan gum samples were exposed to ultrasound irradiation from 30 min to 120 min. Intensity ratio of signal *a* to signal *c* (proton of pyruvate) was similarly reduced, indicating a scission event that occurs at the side chain of xanthan polymer. This event was likely since the side chains of xanthan polymer in salt-free aqueous solution are made to extend from high repulsive forces between the side chains and polymer backbone.

A comparison was made between xanthan gum samples in salt-free and 0.1 M NaCl solutions, exposed to 30 min ultrasound irradiation. The addition of electrolyte causes a reduction in the degree of degradation as mentioned previously; hence the signal intensities of both *a:b* and *a:c* were expected to be higher in 0.1 M NaCl solution as compared to salt-free solution since less degradation would have occurred. However, from Figure 4.14, it was observed that in the presence of salt, the ratio intensities of these two side chain components were lower. It is suggested that the addition of NaCl in the xanthan aqueous solution led to a highly ordered helical conformation in the polymer from the folding of the side chains, hence reducing the signals of available acetate and pyruvate protons.

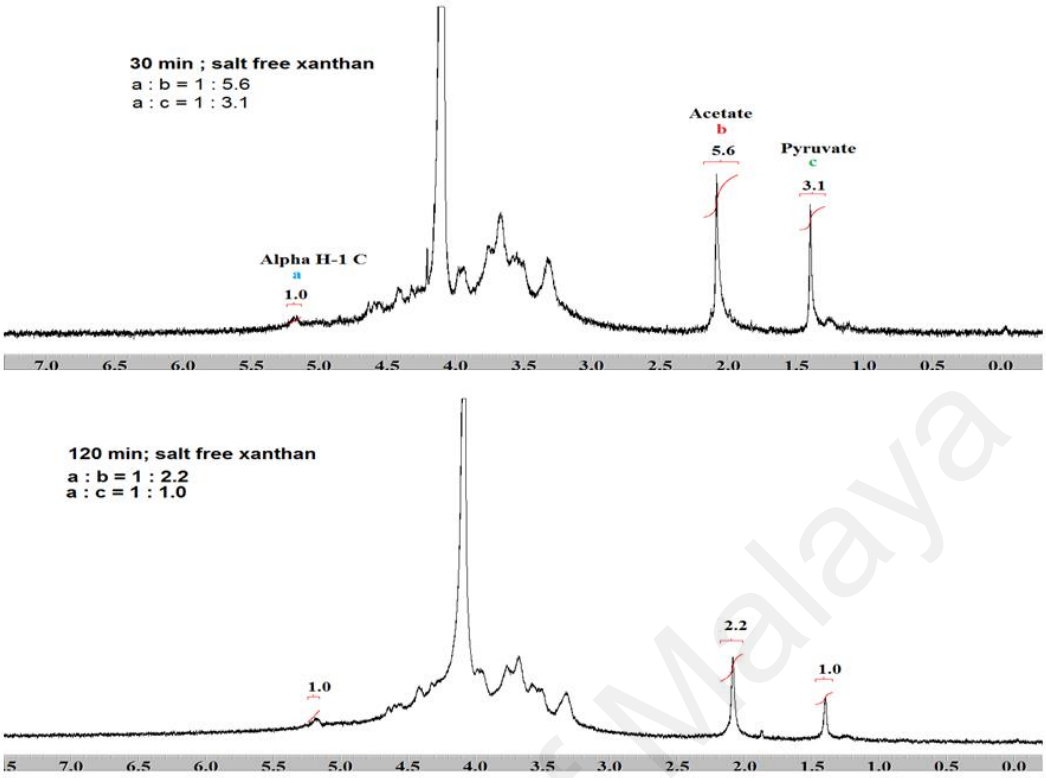

Figure 4.13 ^{1}H NMR spectra of sonicated xanthan gum samples in salt free solutions exposed to 11.5 W cm^{-2} power intensity

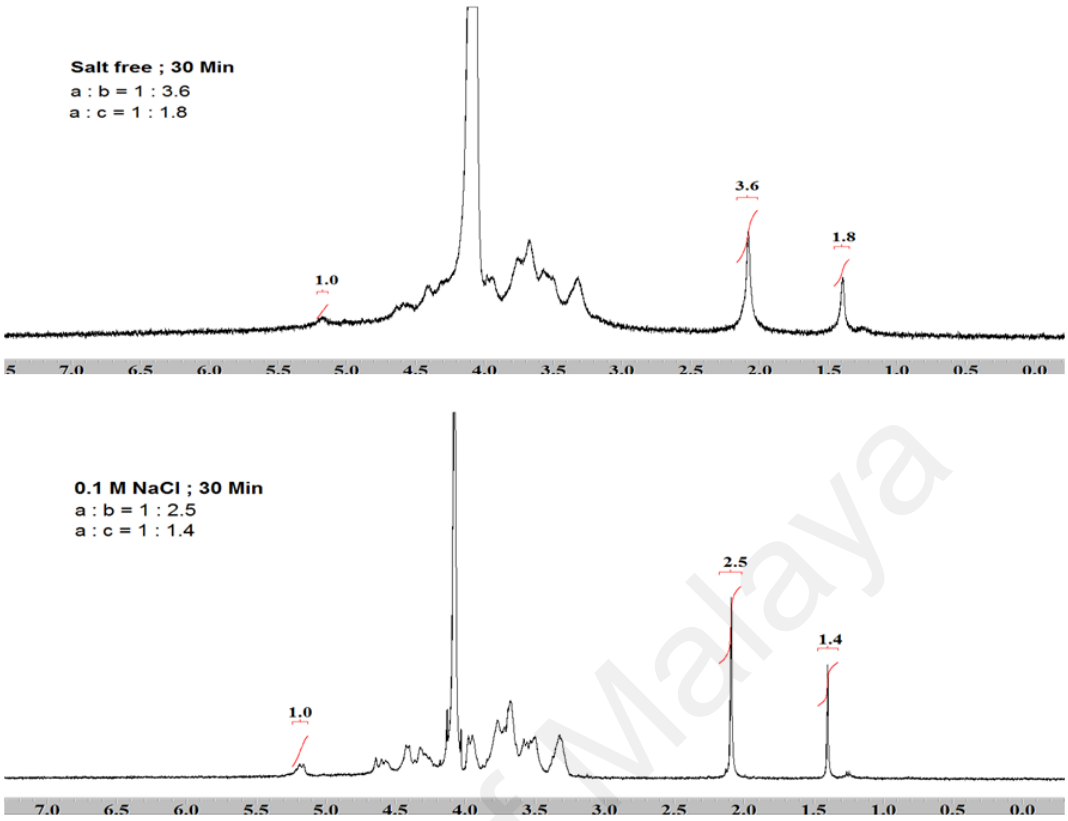

Figure 4.14 ^{1}H NMR spectra of sonicated xanthan gum samples in solutions with different NaCl concentrations exposed to 11.5 W cm^{-2} power intensity

CHAPTER 5

CONCLUSIONS

The extent of the xanthan polymer degradation by sonication was clearly dependent upon polymer concentration and ionic strength of its aqueous solution. Efficient ultrasound-mediated degradation was achieved in dilute polymer concentration and very low ionic strength or salt free solution with xanthan polymer subjected to mid-point chain scission along its length. Side chain of the polymer is proposed to be the primary site of scission action when irradiated with ultrasound. This study provided important insights into some fundamental aspects of ultrasound-mediated degradation of xanthan polymer.

FUTURE WORK

The fundamental understanding obtained from the current research is invaluable for efficient and practical future functionalization of biopolymer through controlled degradation process, which could provide numerous types of platform chemicals. It would also provide future research with important baseline knowledge in designing a working system for controlled industrial degradation of biopolymer.

6.0 BIBLIOGRAPHY

Asgharzadehahmadi, S., Abdul Raman, A. A., Parthasarathy, R., & Sajjadi, B. (2016). Sonochemical reactors: Review on features, advantages and limitations. *Renewable and Sustainable Energy Reviews, 63*, 302-314.

Benny, I. S., Gunasekar, V., & Ponnusami, V. (2014). Review on application of xanthan gum in drug delivery. *International Journal of PharmTech Research, 6*, 1322-1326.

Bradshaw, I., Nisbet, B., Kerr, M., & Sutherland, I. (1983). Modified xanthan-its preparation and viscosity. *Carbohydrate Polymers, 3*(1), 23-38.

Camesano, T. A., & Wilkinson, K. J. (2001). Single molecule study of xanthan conformation using atomic force microscopy. *Biomacromolecules, 2*(4), 1184-1191.

Capron, I., Brigand, G., & Muller, G. (1997). About the native and renatured conformation of xanthan exopolysaccharide. *Polymer, 38*(21), 5289-5295.

Cheetham, N. W., & Mashimba, E. N. (1991). Characterisation of some enzymic hydrolysis products of xanthan. *Carbohydrate Polymers, 15*(2), 195-206.

Christensen, B. E., Myhr, M. H., & Smidsrød, O. (1996). Degradation of double-stranded xanthan by hydrogen peroxide in the presence of ferrous ions: Comparison to acid hydrolysis. *Carbohydrate Research, 280*(1), 85-99.

Christensen, B. E., & Smidsrød, O. (1991). Hydrolysis of xanthan in dilute acid: Effects on chemical composition, conformation, and intrinsic viscosity. *Carbohydrate Research, 214*(1), 55-69.

Christensen, B. E., Smidsroed, O., Elgsaeter, A., & Stokke, B. T. (1993). Depolymerization of double-stranded xanthan by acid hydrolysis: Characterization of partially degraded double strands and single-stranded oligomers released from the ordered structures. *Macromolecules, 26*(22), 6111-6120.

Chun, M. S., & Park, O. O. (1994). On the intrinsic viscosity of anionic and nonionic rodlike polysaccharide solutions. *Macromolecular Chemistry and Physics, 195*(2), 701-711.

Ciesielski, W., & Tomasik, P. (2008). Metal complexes of xanthan gum. *Electronic Journal of Polish Agricultural Univeristies, 11*(2), 25.

Czechowska-Biskup, R., Rokita, B., Lotfy, S., Ulanski, P., & Rosiak, J. M. (2005). Degradation of chitosan and starch by 360-kHz ultrasound. *Carbohydrate Polymers, 60*(2), 175-184.

Dário, A. F., Hortêncio, L. M. A., Sierakowski, M. R., Neto, J. C. Q., & Petri, D. F. S. (2011). The effect of calcium salts on the viscosity and adsorption behavior of xanthan. *Carbohydrate Polymers, 84*(1), 669-676.

Einbu, A., & Vårum, K. M. (2003). Structure–property relationships in chitosan. In P. Tomasik (Ed.), *Chemical and functional properties of food saccharides* (pp. 217-227). Florida: CRC Press.

Faïd, F., Contamine, F., Wilhelm, A. M., & Delmas, H. (1998). Comparison of ultrasound effects in different reactors at 20 kHz. *Ultrasonics Sonochemistry, 5*(3), 119-124.

Faria, S., de Oliveira Petkowicz, C. L., de Morais, S. A. L., Terrones, M. G. H., de Resende, M. M., de França, F. P., & Cardoso, V. L. (2011). Characterization of xanthan gum produced from sugar cane broth. *Carbohydrate Polymers, 86*(2), 469-476.

Fitzpatrick, P., Meadows, J., Ratcliffe, I., & Williams, P. A. (2013). Control of the properties of xanthan/glucomannan mixed gels by varying xanthan fine structure. *Carbohydrate Polymers, 92*(2), 1018-1025.

Galindo, E., & Albiter, V. (1996). High-yield recovery of xanthan by precipitation with isopropyl alcohol in a stirred tank. *Biotechnology Progress, 12*(4), 540-547.

García-Ochoa, F., Santos, V., & Alcón, A. (1997). Xanthan gum production in a laboratory aerated stirred tank bioreactor. *Chemical and Biochemical Engineering Quarterly, 11*(2), 69-74.

García-Ochoa, F., Santos, V. E., Casas, J. A., & Gómez, E. (2000). Xanthan gum: Production, recovery, and properties. *Biotechnology Advances, 18*(7), 549-579.

Gonzales, R., Johns, M., Greenfield, P., & Pace, G. (1989). Xanthan gum precipitation using ethanol. *Process Biochemistry, 24*(6), 200-203.

Grönroos, A., Pirkonen, P., Heikkinen, J., Ihalainen, J., Mursunen, H., & Sekki, H. (2001). Ultrasonic depolymerization of aqueous polyvinyl alcohol. *Ultrasonics Sonochemistry, 8*(3), 259-264.

Harkal, U., Gogate, P., Pandit, A., & Shenoy, M. (2006). Ultrasonic degradation of poly (vinyl alcohol) in aqueous solution. *Ultrasonics Sonochemistry, 13*(5), 423-428.

He, Y. W., & Zhang, L. H. (2008). Quorum sensing and virulence regulation in *Xanthomonas campestris*. *FEMS Microbiology Reviews, 32*(5), 842-857.

Holzwarth, G. (1976). Conformation of the extracellular polysaccharide of *Xanthomonas campestris. Biochemistry, 15*(19), 4333-4339.

Holzwarth, G., & Prestridge, E. (1977). Multistranded helix in xanthan polysaccharide. *Science, 197*(4305), 757-759.

Hsiao, Y. M., Liao, H. Y., Lee, M. C., Yang, T. C., & Tseng, Y. H. (2005). Clp upregulates transcription of engA gene encoding a virulence factor in *Xanthomonas campestris* by direct binding to the upstream tandem Clp sites. *FEBS Letters, 579*(17), 3525-3533.

Huang, C., Miao, M., Janaswamy, S., Hamaker, B. R., Li, X., & Jiang, B. (2015). Polysaccharide modification through green technology: Role of endodextranase in improving the physicochemical properties of (1→3)(1→6)-α-d-Glucan. *Journal of Agricultural and Food Chemistry, 63*(28), 6450-6456.

Ikeda, S., Gohtani, S., Nishinari, K., & Zhong, Q. (2012). Single molecules and networks of xanthan gum probed by atomic force microscopy. *Food Science and Technology Research, 18*(5), 741-745.

Kalogiannis, S., Iakovidou, G., Liakopoulou-Kyriakides, M., Kyriakidis, D. A., & Skaracis, G. N. (2003). Optimization of xanthan gum production by *Xanthomonas campestris* grown in molasses. *Process Biochemistry, 39*(2), 249-256.

Kasaai, M. R. (2013). Input power-mechanism relationship for ultrasonic irradiation: food and polymer applications. *Natural Science, 5*, 14-22.

Kasaai, M. R., Arul, J., & Charlet, G. (2008). Fragmentation of chitosan by ultrasonic irradiation. *Ultrasonics Sonochemistry, 15*(6), 1001-1008.

Katzbauer, B. (1998). Properties and applications of xanthan gum. *Polymer Degradation and Stability, 59*(1), 81-84.

Kitamura, S., Takeo, K., Kuge, T., & Stokke, B. T. (1991). Thermally induced conformational transition of double-stranded xanthan in aqueous salt solutions. *Biopolymers, 31*(11), 1243-1255.

Koda, S., Taguchi, K., & Futamura, K. (2011). Effects of frequency and a radical scavenger on ultrasonic degradation of water-soluble polymers. *Ultrasonics Sonochemistry, 18*(1), 276-281.

Kool, M. M., Gruppen, H., Sworn, G., & Schols, H. A. (2013a). Comparison of xanthans by the relative abundance of its six constituent repeating units. *Carbohydrate Polymers, 98*(1), 914-921.

Kool, M. M., Gruppen, H., Sworn, G., & Schols, H. A. (2014). The influence of the six constituent xanthan repeating units on the order-disorder transition of xanthan. *Carbohydrate Polymers, 104*, 94-100.

Kool, M. M., Schols, H. A., Delahaije, R. J., Sworn, G., Wierenga, P. A., & Gruppen, H. (2013b). The influence of the primary and secondary xanthan structure on the enzymatic hydrolysis of the xanthan backbone. *Carbohydrate Polymers, 97*(2), 368-375.

Lambert, F., & Rinaudo, M. (1985). On the thermal stability of xanthan gum. *Polymer, 26*(10), 1549-1553.

Leela, J., & Sharma, G. (2000). Studies on xanthan production from *Xanthomonas campestris*. *Bioprocess Engineering, 23*(6), 687-689.

Li, R., & Feke, D. L. (2015). Rheological and kinetic study of the ultrasonic degradation of xanthan gum in aqueous solutions. *Food Chemistry, 172*, 808-813.

Liu, H., Bao, J., Du, Y., Zhou, X., & Kennedy, J. F. (2006). Effect of ultrasonic treatment on the biochemphysical properties of chitosan. *Carbohydrate Polymers, 64*(4), 553-559.

Liu, H., Huang, C., Dong, W., Du, Y., Bai, X., & Li, X. (2005). Biodegradation of xanthan by newly isolated *Cellulomonas* sp. LX, releasing elicitor-active xantho-oligosaccharides-induced phytoalexin synthesis in soybean cotyledons. *Process Biochemistry, 40*(12), 3701-3706.

Liu, W., Sato, T., Norisuye, T., & Fujita, H. (1987). Thermally induced conformational change of xanthan in 0.01 M aqueous sodium chloride. *Carbohydrate Research, 160*, 267-281.

Lorimer, J., & Mason, T. (2002). *Applied Sonochemistry: Uses of power ultrasound in chemistry and processing*. Federal Republic of Germany: Wiley-VCH.

Lu, G. T., Yang, Z. J., Peng, F. Y., Tan, Y. N., Tang, Y. Q., Feng, J. X., Tang, J. L. (2007). The role of glucose kinase in carbohydrate utilization and extracellular polysaccharide production in *Xanthomonas campestris pathovar campestris*. *Microbiology*, *153*(12), 4284-4294.

Madras, G., Kumar, S., & Chattopadhyay, S. (2000). Continuous distribution kinetics for ultrasonic degradation of polymers. *Polymer Degradation and Stability, 69*(1), 73-78.

Martini, S. (2013). *Sonocrystallization of fats.* New York: Springer-Verlag New York.

Mason, T., Lorimer, J., Bates, D., & Zhao, Y. (1994). Dosimetry in sonochemistry: The use of aqueous terephthalate ion as a fluorescence monitor. *Ultrasonics Sonochemistry*, *1*(2), 91-95.

Mason, T. J., & Lorimer, J. P. (2003a) *Applied sonochemistry: Uses of power ultrasound in chemistry and processing*. German: Wiley-VCH Verlag GmbH & Co. KGaA.

Mason, T. J., & Lorimer, J. P. (2003b). Sonochemistry in environmental protection and remediation in T. J. Mason & J. P. Lorimer (Eds.), *Applied sonochemistry:Uses of power ultrasound in chemistry and processing* (pp. 131-156). German: Wiley-VCH Verlag GmbH & Co. KGaA.

Mason, T. J., & Peters, D. (2002). *Practical sonochemistry: Power ultrasound uses and applications*. Cambridge: Woodhead Publishing.

Matsuda, Y., Biyajima, Y., & Sato, T. (2009). Thermal denaturation, renaturation, and aggregation of a double-helical polysaccharide xanthan in aqueous solution. *Polymer Journal*, *41*(7), 526-532.

Milas, M., Rinaudo, M., Duplessix, R., Borsali, R., & Lindner, P. (1995). Small angle neutron scattering from polyelectrolyte solutions from disordered to ordered xanthan chain conformation. *Macromolecules, 28*(9), 3119-3124.

Milas, M., Rinaudo, M., & Tinland, B. (1986). Comparative depolymerization of xanthan gum by ultrasonic and enzymic treatments. Rheological and structural properties. *Carbohydrate Polymers*, *6*(2), 95-107.

Mirik, M., Demirci, A. S., Gumus, T., & Arici, M. (2011). Xanthan gum production under different operational conditions by *Xanthomonas axonopodis pv vesicatoria* isolated from pepper plant. *Food Science and Biotechnology*, *20*(5), 1243-1247.

Mohod, A. V., & Gogate, P. R. (2011). Ultrasonic degradation of polymers: Effect of operating parameters and intensification using additives for carboxymethyl cellulose (CMC) and polyvinyl alcohol (PVA). *Ultrasonics Sonochemistry, 18*(3), 727-734.

Moholkar, V. S., Choudhury, H. A., Singh, S., Khanna, S., Ranjan, A., Chakma, S., & Bhasarkar, J. (2015). Physical and chemical mechanisms of ultrasound in biofuel synthesis. In Z. Fang, J. L. R. Smith & X. Qi (Eds.), *Production of Biofuels and Chemicals with Ultrasound* (pp. 35-86). Dordrecht: Springer Netherlands.

Morris, V. J., Franklin, D., & I'Anson, K. (1983). Rheology and microstructure of dispersions and solutions of the microbial polysaccharide from *Xanthomonas campestris* (xanthan gum). *Carbohydrate Research, 121*, 13-30.

Navarrete, R., Himes, R., & Seheult, J. (2000). *Applications of xanthan gum in fluid-loss control and related formation damage.* Paper presented at the SPE Permian Basin Oil and Gas Recovery Conference, Midland, Texas.

Palaniraj, A., & Jayaraman, V. (2011). Production, recovery and applications of xanthan gum by *Xanthomonas campestris*. *Journal of Food Engineering, 106*(1), 1-12.

Paradossi, G., & Brant, D. A. (1982). Light scattering study of a series of xanthan fractions in aqueous solution. *Macromolecules, 15*(3), 874-879.

Pelletier, E., Viebke, C., Meadows, J., & Williams, P. (2001). A rheological study of the order–disorder conformational transition of xanthan gum. *Biopolymers, 59*(5), 339-346.

Pilli, S., Bhunia, P., Yan, S., LeBlanc, R., Tyagi, R., & Surampalli, R. (2011). Ultrasonic pretreatment of sludge: A review. *Ultrasonics Sonochemistry, 18*(1), 1-18.

Poletto, M., Ornaghi, H. L., & Zattera, A. J. (2014). Native cellulose: Structure, characterization and thermal properties. *Materials, 7*(9), 6105-6119.

Prajapat, A. L., & Gogate, P. R. (2015). Depolymerization of guar gum solution using different approaches based on ultrasound and microwave irradiations. *Chemical Engineering and Processing: Process Intensification, 88*, 1-9.

Qian, F., An, L., He, X., Han, Q., & Li, X. (2006). Antibacterial activity of xantho-oligosaccharide cleaved from xanthan against phytopathogenic *Xanthomonas campestris pv. campestris*. *Process Biochemistry, 41*(7), 1582-1588.

Rinaudo, M., Milas, M., Lambert, F., & Vincendon, M. (1983). Proton and carbon-13 NMR investigation of xanthan gum. *Macromolecules, 16*(5), 816-819.

Roller, S., & Jones, S. A. (1996). *Handbook of fat replacers*. New York: CRC Press.

Rosalam, S., & England, R. (2006). Review of xanthan gum production from unmodified starches by *Xanthomonas campestris* sp. *Enzyme and Microbial Technology, 39*(2), 197-207.

Saeman, J. F., Moore, W. E., Mitchell, R. L., & Millett, M. A. (1954). Techniques for the determination of pulp constituents by quantitiative paper chromatography. *Tappi Journal, 37*(8), 336-343.

Saha, D., & Bhattacharya, S. (2010). Hydrocolloids as thickening and gelling agents in food: A critical review. *Journal of Food Science and Technology, 47*(6), 587-597.

Sanderson, G. R. (1981). Applications of xanthan gum. *British Polymer Journal, 13*(2), 71-75.

Sandvik, E., & Maerker, J. (1977). Application of xanthan gum for enhanced oil recovery. *Extracellular Microbial Polysaccharides, 45*, 242-264.

Sato, T., Norisuye, T., & Fujita, H. (1984). Double-stranded helix of xanthan in dilute solution: Evidence from light scattering. *Polymer Journal, 16*(4), 341-350.

Schaefer, M., Icli, B., Weder, C., Lattuada, M., Kilbinger, A. F., & Simon, Y. C. (2016). The role of mass and length in the sonochemistry of polymers. *Macromolecules, 49* (5), 1630-1636.

Schmid, G. (1940). On the kinetics of ultrasonic depolymerization. *Journal of Physical Chemistry, 186*(3), 113-128.

Sharma, Naresh, Dhuldhoya, Merchant, & Merchant. (2006). Xanthan gum - A boon to food industry. *Food Promotion Chronicle, 1*(5), 27-30.

Sharma, A., Gautam, S., & Wadhawan, S. (2014). Xanthomonas In M. L. Tortorello (Ed.), *Encyclopedia of Food Microbiology (Second Edition)* (pp. 811-817). Oxford: Academic Press.

Smith, I. H., & Pace, G. W. (1982). Recovery of microbial polysaccharides. *Journal of Chemical Technology and Biotechnology, 32*(1), 119-129.

Souw, P., & Demain, A. L. (1979). Nutritional Studies on xanthan production by *Xanthomonas campestris* NRRL B1459. *Applied and Environmental Microbiology, 37*(6), 1186-1192.

Stokke, B. T., & Christensen, B. E. (1996). Release of disordered xanthan oligomers upon partial acid hydrolysis of double-stranded xanthan. *Food Hydrocolloids, 10*(1), 83-89.

Stokke, B. T., Elgsaeter, A., Skjrak-Brjek, G., & Smidsrød, O. (1987). The molecular size and shape of xanthan, xylinan, bronchial mucin, alginate, and amylose as revealed by electron microscopy. *Carbohydrate Research, 160*, 13-28.

Suslick, K. S. (1994). Sonochemistry of transition metal compounds. In R. B. King (Ed.), *Encyclopedia of inorganic chemistry* (pp. 3890-3905). New York: J. Wiley & Sons.

Suslick, K. S., & Price, G. J. (1999). Applications of ultrasound to materials chemistry. *Annual Review of Materials Science, 29*(1), 295-326.

Synytsya, A., & Novak, M. (2014). Structural analysis of glucans. *Annals of Translational Medicine, 2*(2), 17-17.

Tako, M., & Nakamura, S. (1989). Evidence for intramolecular associations in xanthan molecules in aqueous media. *Agricultural and Biological Chemistry, 53*(7), 1941-1946.

Tako, M., Tamaki, Y., Teruya, T., & Takeda, Y. (2014). The principles of starch gelatinization and retrogradation. *Food and Nutrition Sciences, 5*, 280-291.

Tiwari, B., Muthukumarappan, K., O'Donnell, C., & Cullen, P. (2010). Rheological properties of sonicated guar, xanthan and pectin dispersions. *International Journal of Food Properties, 13*(2), 223-233.

Trommer, H., & Neubert, R. H. (2005). The examination of polysaccharides as potential antioxidative compounds for topical administration using a lipid model system. *International Journal of Pharmaceutics, 298*(1), 153-163.

Tsaih, M. L., & Chen, R. H. (2003). Effect of degree of deacetylation of chitosan on the kinetics of ultrasonic degradation of chitosan. *Journal of Applied Polymer Science, 90*(13), 3526-3531.

Tul'chinsky, V. M., Zurabyan, S. E., Asankozhoev, K. A., Kogan, G. A., & Khorlin, A. Y. (1976). Study of the infrared spectra of oligosaccharides in the region 1,000 - 40 cm^{-1}. *Carbohydrate Research, 51*(1), 1-8.

Vicente, J. G., & Holub, E. B. (2013). *Xanthomonas campestris pv. campestris* (cause of black rot of crucifers) in the genomic era is still a worldwide threat to brassica crops. *Molecular Plant Pathology, 14*(1), 2-18.

Wolfrom, M. L., & BeMiller, J. N. (1963). *Methods in carbohydrate chemistry: Reactions of carbohydrates* (Vol. 2). New York: Academic Press.

Wu, S. J., Wu, J. H., Xia, L. Z., Chu, C., Liu, D., & Gong, M. (2013). Preparation of xanthan-derived oligosaccharides and their hydroxyl radical scavenging activity. *Carbohydrate Polymers, 92*(2), 1612-1614.

Wu, T., Zivanovic, S., Hayes, D. G., & Weiss, J. (2008). Efficient reduction of chitosan molecular weight by high-intensity ultrasound: Underlying mechanism and effect of process parameters. *Journal of Agricultural and Food chemistry, 56*(13), 5112-5119.

Xiong, X., Li, M., Xie, J., Jin, Q., Xue, B., & Sun, T. (2013). Antioxidant activity of xanthan oligosaccharides prepared by different degradation methods. *Carbohydrate Polymers, 92*(2), 1166-1171.

Xiong, X., Li, M., Xie, J., Xue, B., & Sun, T. (2014). Preparation and antioxidant activity of xanthan oligosaccharides derivatives with similar substituting degrees. *Food Chemistry, 164*, 7-11.

Young, S. L., Martino, M., Kienzle-Sterzer, C., & Torres, J. A. (1994). Potentiometric titration studies on xanthan solutions. *Journal of the Science of Food and Agriculture, 64*(1), 121-127.

Yuen, S.N., Choi, S.M., Phillips, D. L., & Ma, C.Y. (2009). Raman and FTIR spectroscopic study of carboxymethylated non-starch polysaccharides. *Food Chemistry, 114*(3), 1091-1098.

Zatz, J. L. (1984). Applications of gums in pharmaceutical and cosmetic suspensions. *Industrial & Engineering Chemistry Product Research and Development, 23*(1), 12-16.